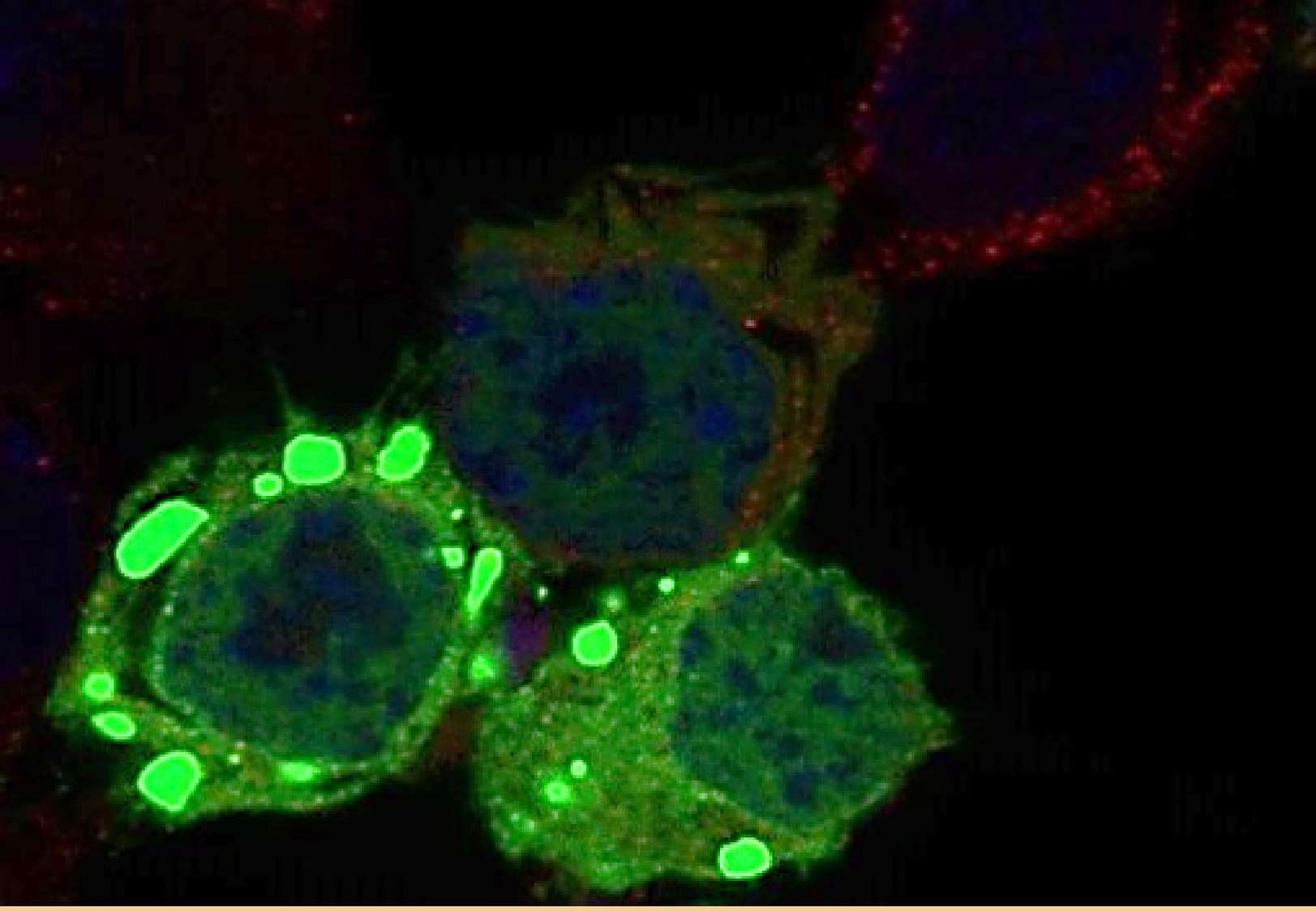

Marco António Rodrigues Ferreira

PERK inhibition role in Spinocerebellar ataxias

Dissertação de Mestrado em Biotecnologia Farmacêutica, orientada pelo Doutor Clévio Nóbrega (CNC) e pelo Professor Doutor Luís Pereira de Almeida e apresentada à Faculdade de Farmácia da Universidade de Coimbra

Setembro 2016

· U C ·

Universidade de Coimbra

Marco António Rodrigues Ferreira

PERK inhibition role in Spinocerebellar ataxias

Dissertação de Mestrado em Biotecnologia Farmacêutica, orientada pelo Doutor Clévio Nóbrega (CNC) e pelo Professor Doutor Luís Pereira de Almeida e apresentada à Faculdade de Farmácia da Universidade de Coimbra

Setembro 2016

· U C ·

UNIVERSIDADE DE COIMBRA

Front cover composed of confocal microscopic image of Neuro2A cells transfected with GFP-MUT ataxin-3 and stained with DAPI and PABP, using 63x objective.

The present work was performed in the Viral Vectors and Gene Therapy group of the Center for Neurosciences and Cell Biology (University of Coimbra, Portugal), leaded by Professor Luís Pereira de Almeida, and under supervision of Clévio Nóbrega

Acknowledgments/Agradecimentos

Após o final desta etapa, não posso deixar de agradecer às pessoas que fizeram parte dela.

Queria agradecer a todos os Professores que me transmitiram os seus ensinamentos, quer da licenciatura, quer do Mestrado, e também à Universidade de Coimbra.

Ao Professor Doutor Luís Pereira de Almeida, por me ter recebido no seu grupo de trabalho, pela disponibilidade, simpatia inigualável e ensinamentos transmitidos.

À Professora Doutora Cláudia Cavadas, por me ter acolhido no seu laboratório, pela simpatia, pela disponibilidade e pela enorme boa disposição que sempre apresentou.

Ao Doutor Clévio Nóbrega, por ter apostado em mim como um aluno capaz de corresponder às suas exigências, por me ter dado a oportunidade de fazer parte deste projeto de investigação, pelos ensinamentos que transmitiu, pela enorme disponibilidade que proporcionou e pela paciência em algumas situações. Obrigado por tudo!

À Sara Silva, por todo o apoio prestado e por me orientar e ensinar praticamente tudo o que sei fazer em laboratório, pela enorme paciência e pela simpatia. Não posso deixar de agradecer também à Mariana Botelho, à Marisa Ferreira, Célia Aveleira e Patrícia, que estiveram presentes para tudo o que precisei. Obrigada pela vossa disponibilidade e amizade.

A todo o grupo do Professor Luís Almeida, por me terem recebido tão bem, pela vossa simpatia e disponibilidade. Em especial: à Janete, Sara, Dina, Ana, Filipa, Vítor e Carlos pelos ensinamentos e pela enorme boa disposição no laboratório criada por todos vocês.

Aos meus companheiros de laboratório e estudantes de mestrado, Sandra Tomé e João Cruzeiro, por terem estado sempre ao meu lado, por todo o apoio dado, ensinamentos, pelas conversas, risadas, almoços e por terem tornado este ano letivo um ano memorável.

A todos os colegas e amigos de investigação que fizeram parte desta jornada, um muito obrigado. Um especial obrigado à simpatia e motivação proporcionada pela Joana Saraiva.

E finalmente, à minha família, namorada e amigos. À minha namorada, por ser a minha melhor amiga, a minha confidente e me chatear a cabeça sempre que precisei. À minha mãe e irmão que me apoiaram em tudo aquilo que puderam e que sempre estiveram presentes. Aos meus avós e tios pelo enorme apoio, e que sem eles nenhum destes cinco anos de vivências seriam possíveis, são os meus segundos pais. Obrigado por acreditarem em mim e me terem dado esta oportunidade na minha vida. Por último um obrigado a todos os meus amigos que estiveram sempre presentes, apoio não faltou da vossa parte. Obrigado a todos!

Index

List of Figures

List of Tables

Abbreviations

5-FU – 5-Fluorouracil

A1 – Adenosine receptors 1

A2BP1 – Ataxin-2-binding protein

A3 – Adenosine receptors 3

AD – Alzheimer's Disease

ALS – Amniotrophic Lateral Sclerosis

ANG – Angiogenenin

ATP – Adenosine Triphosphate

ATXN2 – Ataxin-2

ATXN3 – Ataxin-3

BRF1 – Butyrate response factor 1

BSA – Bovine serum albumin

CACNAIA – α1A Ca^{+2} channel

CAG – Cytosine-Adenine-Guanine

CHX – Ciclohexamide

CNC – Centre for Neuroscience and Cell Biology

CPEB – Cytoplasmic polyadenylation element-binding protein

DAPI – 4',6-diamidino-2-phenylindole

DARP-32 – Cyclic AMP-regulated phosphoprotein, relative molecular mass 32.000

DMEM – Dulbecco's modified Eagle's medium supplemented

DMSO – Dimethyl sulfoxide

DNA – Deoxyribonucleic acid

DRPLA – Dentarubralpallidoluysian atrophy

DYRK3 – Tyrosine-phosphorylation-regulated kinase 3

ECF – Enhanced Chemifluorescent substrate

eIF – Eukaryotic translation initiation factor

eIF2α – Eukaryotic translation initiation factor 2 alpha

ER – Endoplasmic reticulum

eRF1 – Eukaryotic release factor 1

eRF3 – Eukaryotic release factor 3

FAST – Fas-activted serine/threonine kinase

FBP – FUSE-binding protein

FBS – Fetal bovine serum

FCCP – Carbonyl cyanide p-(trifluoromethoxy)-phenylhydrazon

FMRP – Fragile x mental retardation protein

FTLD – Frontotemporal dementia

FUS – Fused in sarcoma

FXR1 – Fragile X mental retardation-related protein 1

G3BP1 – RasGTPase activating protein-binding 1

GCN – General control nonderepressible

GDP – Guanosine diphosphate

GFAP – Glial fibrillary acidic protein

GTP – Guanosine-5'-triphosphate

HD – Huntington's disease

HEK293T – Human embryonic kidney cell line 293T

HRI – Heme-regulated inhibitor kinase

HSP70 – Heat-shock protein 70

IBA-1 – Ionized calcium-binding adapter molecule 1

KSRP – KH-type splicing regulatory protein

LC3 – Light chain 3

LV – Lentiviral

Met – Methionine

MJD – Machado-Joseph disease

mRNA – Messenger RNA

mRNP – Messenger ribonucleoprotein

mTORC1 – mammalian target of rapamycin complex 1

MUT – Mutant

Neuro2A – Mouse neuroblastoma cell line

NT – Non-treated

O-Glc-NAc – O-linked N-acetylglucosamine

OPT – Optineurin

ORF – Open reading frame

P62 – Nucleoporin p62

PABP – Poly(A) Binding Protein

PAM2 – PABPC1-interacting motif-2

PB – Processing bodies

PBS - Phosphate-buffered saline

PEI – Polyethylenimine

PERK – PKR-like endoplasmic reticulum-resident kinase

PERKi – PERK inhibitor (GSK2606414)

PFA – Paraphormaldehyde

PKR – Double-stranded RNA-activated protein kinase

PMRI – Polysome-associated RNAse 1

polyQ - Polyglutamine track

PrP – Prion protein

PVDF – Polyvinylidene difluoride

Q22 – Wild-type ataxin-2

Q58 – Mutant ataxin-2

RBPs – RNA Binding Proteins

RCK – p54

RISC – RNA-induced silencing complexes

RNA – Ribonucleic acid

RNAi – Interference RNA

RRM – RNA recognition motifs

RT – Room temperature

SA – Sodium Arsenite

SBMA – Spinal and bulbar muscular atrophy

SCA1 – Spinocerebellar ataxia type 1

SCA17 – Spinocerebellar ataxia type 17

SCA2 – Spinocerebellar ataxia type 2

SCA3 – Spinocerebellar ataxia type 3

SCA6 – Spinocerebellar ataxia type 6

SCA7 – Spinocerebellar ataxia type 7

SDS – Sodium dodecyl sulfate

SEM – Standard error of the mean

SGs – Stress Granules

shGFP – Short hairpin RNA for GFP

shPERK – Short hairpin RNA for PERK

shRNA – Short hairpin RNA

SMN – Survival of motor neurons

SN – Substantia nigra

SRC3 – Steroid coactivator 3

TBBP – TATA box binding protein

TBS-T – Tris buffered saline

TDP-43 – TAR DNA-binding protein 43

TIA-1 – TIA1 Cytotoxic Granule-Associated RNA Binding Protein 1

TIAR – TIA-1-related

TRAF2 – Tumor necrosis factor receptor-associated factor 2

tRNA – Transfer RNA

TTP – Tristetraprolin

UIM – Ubiquitin interacting motifs

UTR – Untranslated region

UV – Ultraviolet

VCP – Valosin-containing protein

WT – Wild-type

Abstract

Stress Granules (SGs) are ribonucleoprotein (RNP) complexes composed of abortive translation initiation complexes and a host of RNA binding proteins and signaling proteins involved in several aspects of cellular metabolism. Environmental stress, such as: heat shock, UV radiation, viral infection, and oxidative stress - triggers a series of signals, which eventually lead to the formation of stress granules. Early on, it involves phosphorylation of eukaryotic translation initiation factor eIF2α. This phosphorylation is caused by signaling cascades, namely PKR, PERK/PEK, HRI and GCN2 kinases and culminates in translation arrest. It is hypothesized that SGs could have a cytoprotective role, since the knockout of several SGs proteins render cells more vulnerable to stress and the inhibition of eIF2α dephosphorylation protects cells against some forms of stress. However, weather SGs induction may have beneficial effects in neurodegeneration is yet to be addressed.

SGs formation presents a biological pathway that could be vulnerable to the protein aggregates that accumulate in neurodegenerative disease. Ataxin-2 (the gene product of Spinocerebellar Ataxia Type 2) has been shown to co-localize with classic SG markers (TIA-1, TIAR and/or G3BP) in cells undergoing stress. It was shown to be recruited and to play a regulatory role in SGs, by assembling with polysomes and interacting with PABP. It is also known that Ataxin-2 interacts with Ataxin-3, contributing significantly to Spinocerebellar Ataxia Type 3/Machado Joseph's Disease (SCA3/MJD) pathology.

The general purpose of this work was to provide an insight into the role that PERK inhibition might have in neurodegenerative disorders, namely SCA2 and SCA3/MJD, specifically in how the PERK inhibition could influence the causative proteins of these disorders.

We observed that PERK inhibition is able to decrease ataxin-2 and/or ataxin-3 levels, by inducing oxidative stress with sodium arsenite (SA). We also found that PERK inhibition decreases significantly the aggregation of mutant ataxin-3 and/or mutant ataxin-2, and oxidative stress is a prone environment to aggregation in a SCA2 cellular model. *In vivo*, we observed that shPERK expression in mouse striatum of SCA3/MJD lentiviral model increase significant the loss of neuronal markers, and neuronal death were observed. Future studies need to be performed in order to clarify the role of PERK inhibition in the neurodegeneration context.

Keywords: Stress Granules, SCA2, Ataxin-2, SCA3/MJD, Ataxin-3, eIF2alpha, PERK inhibition, Sodium arsenite

Resumo

Os grânulos de *stress* (SGs) são complexos de nucleoproteínas que contêm RNA (RNP), proteínas presentes na iniciação da tradução, proteínas ligadoras de RNA e proteínas envolvidas em vários aspetos do metabolismo celular. Condições de stress, tais como: choque térmico, radiação UV e stress oxidativo - levam à formação de grânulos de *stress*. Esta via inicia-se com a fosforilação do eIF2α, provocada por algumas cascatas de sinalização, nomeadamente PKR, PERK/PEK, HRI e GCN2 e culmina na inibição do processo de tradução. Está formulada a hipótese de que os SGs possam ter um papel cito-protetor, dado que o silenciamento de algumas proteínas dos SGs torna as células mais vulneráveis ao *stress* e que a inibição da fosforilação do eIF2α protege as células contra algumas formas de *stress*. Contudo, a hipótese de que os SGs possam ter um efeito benéfico no contexto degenerativo ainda está por ser clarificada.

A formação de SGs apresenta uma via biológica que pode ser vulnerável aos agregados proteicos que se acumulam nas doenças neurodegenerativas. A ataxina-2 [forma mutada causa Ataxia Espinocerebelosa Tipo 2 (SCA2)] co-localiza com marcadores de SGs (TIA-1, TIAR e / ou G3BP) em células submetidas a stress. Foi ainda mostrado que esta proteína pode ser recrutada e desempenhar um papel regulador nos SGs, através da interação com polissomas e com o PABP. Sabe-se que ataxina-2 interage com ataxina-3, contribuindo significativamente para a patologia da Ataxia Espinocerebelosa Tipo 3/Doença de Machado-Joseph (SCA3/MJD).

O objetivo geral deste trabalho é fornecer uma compreensão do papel da inibição da PERK nas doenças neurodegenerativas, nomeadamente SCA2 e SCA3/MJD, especificamente o modo como esta inibição poderia influenciar as proteínas causadoras destas patologias (ataxina-2 e ataxina-3).

Observou-se que a inibição da PERK diminui os níveis de ataxina-2 e / ou ataxina-3, por indução de *stress* oxidativo com o arsenito de sódio (SA). A inibição da PERK também diminui significativamente a agregação de ataxina-3 mutante e / ou ataxina-2 mutante, sendo que o *stress* oxidativo induzido constitui um ambiente propenso à agregação no modelo celular de SCA2. Em ratinhos, observou-se que a expressão do shPERK (short hairpin para PERK) leva a um aumento significativo de perda de marcadores neuronais, no estriado de ratinho num modelo lentiviral de SCA3. Foi também observada morte neuronal neste tratamento. No futuro serão necessários estudos adicionais para clarificar o papel da inibição da PERK num contexto de neurodegeneração.

Palavras-chave: Grânulos de *Stress*, SCA2, Ataxina-2, SCA3/MJD, Ataxina-3, eIF2alpha, inibição da PERK, Arsenito de sódio

CHAPTER 1 – INTRODUCTION

1.1 Eukaryotic Translation

The process of protein synthesis from amino acid sequences specified by the sequence of codons in messenger RNA is called translation (represented in Fig.1). Translation is crucial and the first stage of protein biosynthesis.

Protein biosynthesis is mainly regulated at the initiation stage, allowing rapid, reversible and spatial control of gene expression. Progress over recent years in determining the structures and activities of initiation factors, and in mapping their interactions in ribosomal initiation complexes, have advanced the understanding of the complex translation initiation process (Jackson, Hellen and Pestova, 2010; Hinnebusch, 2014). The first step in the initiation pathway is the assembly of the eIF2-GTP-Met-tRNAi ternary complex. The ternary complex binds to the small (40S) ribosomal subunit. This binding is facilitated by (at least) eIFs 1, 1α, and 3, resulting in the 43S complex (Kapp and Lorsch, 2004). The 43S complex then scans the 5′ untranslated region (5′ UTR) in the 5′ to 3′ direction to the initiation codon. After initiation codon recognition and 48S complex formation, eIF5 and eIF5B promote the hydrolysis of eIF2-bound GTP, the displacement of eIFs and the joining of a 60S subunit. Although most mRNAs use the scanning mechanism, initiation on a few mRNAs is mediated by internal ribosome entry sites (Jackson, Hellen and Pestova, 2010).

Following translation initiation, an 80S ribosome contacts with a messenger RNA (mRNA) with the anticodon of Met-tRNA$_i$ in the P site base-paired with the start codon. The second codon of the open reading frame (ORF) is present in the A (acceptor) site of the ribosome awaiting binding of the cognate aminoacyl-tRNA. The eukaryotic elongation factor eEF1A, binds aminoacyl-tRNA in a GTP-dependent manner and then directs the tRNA to the A site of the ribosome. Codon recognition by the tRNA triggers GTP hydrolysis by eEF1A, releasing the factor and enabling the aminoacyl-tRNA to be accommodated into the A site (Dever and Green, 2012). Codon-anticodon base pairing induces three bases in the small ribosomal subunit's rRNA to swing out and interact with the resulting mRNA-tRNA duplex. This in turn appears GTPase activity. eEF1α-GDP releases the aminoacyl tRNA into the A site in form that can continue with peptide bond formation. The ribosomal peptidyl transferase center then catalyses the formation of a peptide bond between the incoming amino acid and the peptidyl tRNA. The result is a deacylated tRNA in a hybrid state with its acceptor end in the exit (E) site of the large ribosomal subunit and its anticodon end in the P site of the small subunit. The peptidyl-tRNA is in a similar hybrid situation with its acceptor

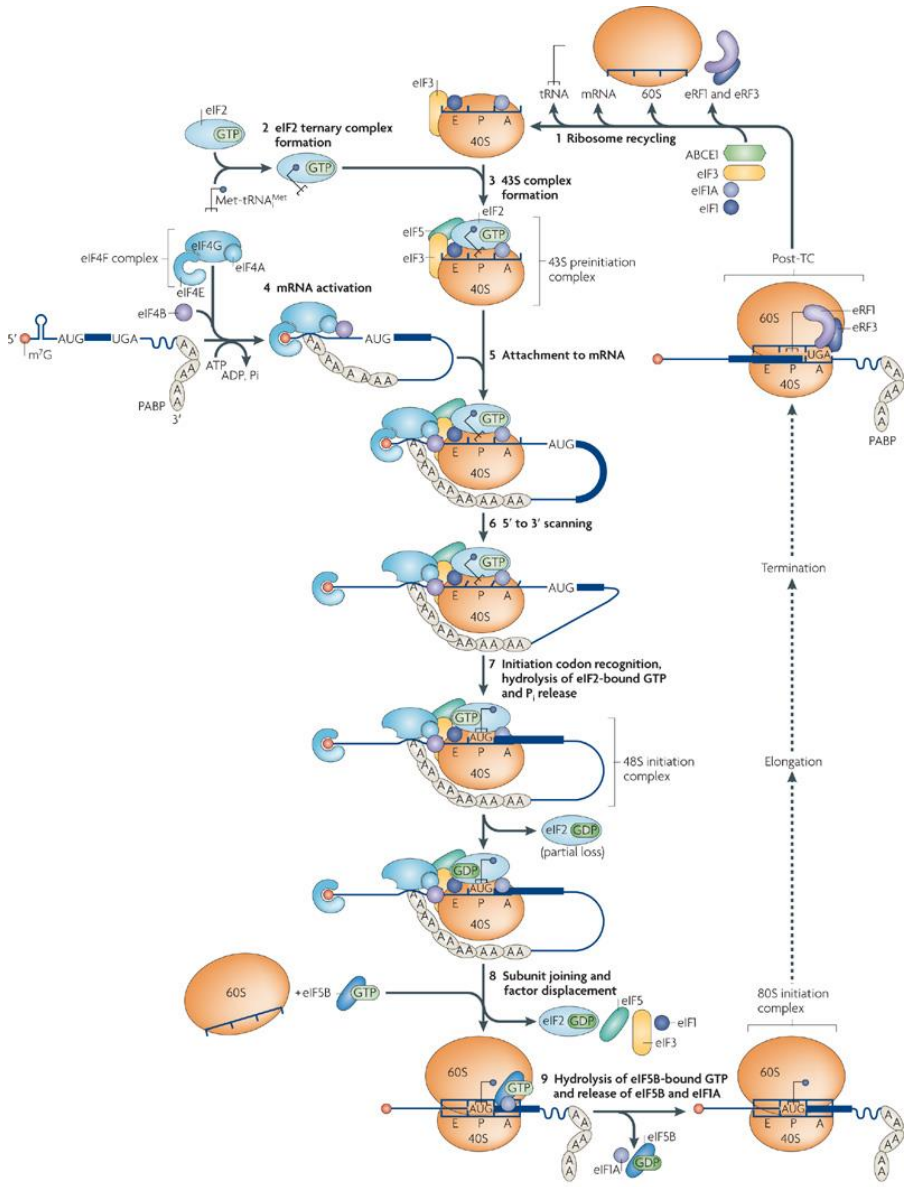

Figure 1 - Model of the canonical pathway of eukaryotic translation initiation. The canonical pathway of eukaryotic translation initiation is divided into eight stages (2–9). These stages are: eukaryotic initiation factor 2 (eIF2)–GTP–Met-tRNAMet i ternary complex formation (2); formation of a 43S preinitiation complex (3); mRNA activation (4); attachment of the 43S complex to this mRNA region (5); scanning of the 5′ UTR in a 5′ to 3′ direction by 43S complexes (6); recognition of the initiation codon and 48S initiation complex formation (7); joining of 60S subunits to 48S complexes (8); and GTP hydrolysis by eIF5B and release of eIF1A and GDP-bound eIF5B from assembled elongation competent 80S ribosomes (9). Translation is a cyclical process, in which termination follows elongation and leads to recycling (1), (adapted from Jackson, Hellen and Pestova, 2010).

end in the P site of the large subunit and its anticodon end in the A site of the small subunit. This complex must be translocated such that the deacylated tRNA is completely in the E site, the peptidyl tRNA completely in the P site, and the mRNA moved by three nucleotides to place the next codon of the mRNA into the A site. This task is accomplished by elongation factor 2, which hydrolyzes GTP as it facilitates translocation. This cycle is repeated until a stop codon is encountered and the process of termination is initiated. Following the hydrolysis of GTP and the release of aminoacyl tRNA onto the ribosome,

eEF1α-GDP is released and must be recycled to its GTP-bound form (Kapp and Lorsch, 2004; Dever and Green, 2012).

The last phase of translation is termination. These phase occurs when one of the three termination codons (UAA, UGA, UAG) moves into the A site. These codons are not recognized by any tRNAs. Termination of elongation is dependent on eukaryotic release factors: there is only two release factors that are eRF1 and eRF3, which recognizes all three stop codons (Kapp and Lorsch, 2004; Dabrowski, Bukowy-bieryllo and Zietkiewicz, 2015; Nick J. Proudfoot, 2016).

1.2 Cellular stress response

Stress granules (SGs) are not seen in cells growing under favourable conditions but are rapidly induced in response to environmental stress. Experimental stress conditions that induce SGs include oxidative stress induced by arsenite or H_2O_2, osmotic shock induced by exposure to sorbitol, mitochondrial stress induced by carbonyl cyanide p-(trifluoromethoxy)-phenylhydrazon (FCCP) or clotrimazole, UV irradiation, viral infection, cellular acidosis and thermal stress (Kedersha and Anderson, 2007; Chudinova, Nadezhdina and Ivanov, 2012; Hofmann *et al.*, 2012, 2012; Lloyd, 2012). These toxic environmental stimuli impair translation initiation via an eIF2α-dependent or independent pathway, ultimately leading to translational arrest.

eIF2α-dependent SG assembly is induced when stress stimuli activate specific serine/threonine kinases (PKR, PERK, HRI, GCN) (Anderson and Kedersha, 2009). These kinases subsequently phosphorylate and thereby inactivate the α subunit of eIF2 (Fig. 2), which is usually required for translation initiation in its unphosphorylated state.

Phosphorylation of eIF2α results in decreased production of the ternary complex composed of eIF2-GTP-tRNAiMet, which must bind to the 40S small ribosomal subunit to initiate mRNA scanning and start codon selection. As a result of the decreased availability of eIFs and ternary complexes, further rounds of translation cannot be initiated (Anderson and Kedersha, 2007).

Some chemical compounds (e.g. hippuristanol, pateamine A) initiate SG assembly independently of eIF2α. They interfere with translation initiation by blocking eIF4A helicase, which is required for the ribosome recruitment phase of translation initiation (Bentmann, Haass e Dormann, 2013).

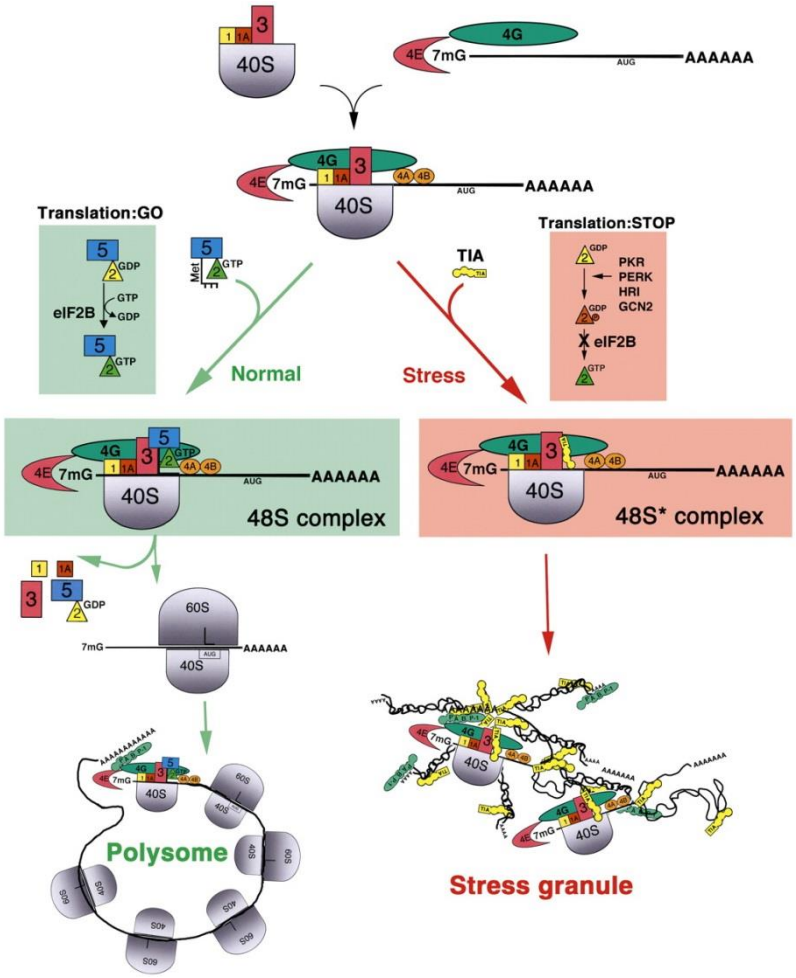

Figure 2 - Translational initiation in the absence or presence of stress. (Green panels) In the absence of stress. When the eIF2-GTP-tRNAMet ternary complex is available, a canonical 48S preinitiation complex is assembled at the 5′ end of capped transcripts (green arrow: Normal). Ribosomes are added to the transcript; the mRNA is converted into a polysome. (Red panels) In stressed cells (red arrow: Stress), phosphorylation of eIF2α by PKR, PERK, HRI or GCN2. Under these conditions, TIA-1 is included in a non-canonical. TIA-1 self-aggregation then promotes the accumulation of these complexes at discrete cytoplasmic foci known as stress granules (adapted from Anderson and Kedersha, 2002).

In stress conditions, eukaryotic cells reprogram mRNA metabolism to repair stress-induced damage and adapt to changed conditions. During this process, the translation of mRNAs encoding "housekeeping" proteins is inhibited, whereas the translation of mRNAs encoding molecular chaperones and enzymes involved in damage repair is enhanced (Anderson and Kedersha, 2006).

Several proteins act downstream of phospho-eIF2α to potentiate or inhibit SG assembly. Self-aggregation of either TIA proteins or G3BP1 promotes SG assembly. Stress-induced aggregation of TIA proteins is mediated by a glutamine-rich prion like domain that is regulated by HSP70 (Gilks *et al.*, 2004). Similarly, self-aggregation of the RNA-binding protein G3BP1 promotes SG assembly, a process that is regulated by phosphorylation at serine 149 (Mouaikel, Geer and Tazi, 2001; Anderson and Kedersha, 2006). Although not present in

SGs, the mitochondria associated apoptosis-inducing factor inhibits SG assembly by shifting the cellular redox potential (Candé *et al.*, 2004). Finally, various mitochondrial poisons induce SGs, suggesting a requirement for ATP in either SG assembly or disassembly (Kedersha *et al.*, 2000, 2005). Thus, SG assembly/disassembly is regulated by numerous signalling pathways acting downstream of phospho-eIF2α.

SGs are also detectable in tissues from stressed animals. In chickens treated with the ototoxic antibiotic gentamycin, the appearance of SGs in cochlear cells (Mangiardi *et al.*, 2004) occurs several hours before the onset of apoptosis. In another study, whole-animal radiotherapy induces SG assembly within individual tumor cells (Moeller *et al.*, 2004), in which the radiation-induced translation of hypoxia inducible factor–1α- regulated transcripts is delayed pending SG disassembly during recovery, suggesting that the expression of these transcripts is inhibited by their retention in SGs. Similar results have been described using an animal model of stroke, in which SGs may regulate protein translation in neurons during ischemia (Kayali, Montie and Rafols, 2005). These studies indicate that SGs are not *in vitro* artefacts of cell culture but are an integral part of the organism response to stress.

1.3 Stress granules

Stress granules are cytoplasmic mRNPs that form when translation initiation is impaired, either due to decreased translation initiation rates during a stress response, the addition of drugs blocking translation initiation, knockdown of specific initiation factors, or overexpression of RNA binding proteins that repress translation (Buchan and Parker, 2009; Cohen *et al.*, 2013). These cellular structures seem to be in a dynamic equilibrium with polysomes as well and assemble and disassemble very rapidly in the cytoplasm of plant and mammalian cells after being subjected to environmental stresses (Anderson and Kedersha, 2006). During these stress conditions, the translation of housekeeping genes is arrested and untranslated mRNA accumulates in SGs (Nonhoff *et al.*, 2007).

Although there are many types of RNA granules (e.g. Stress Granules, P-bodies, germ granules, neuronal granules, nuclear paraspeckles), SGs and P-bodies are the best understood and closely associated with a variety of diseases. The classification of RNA granules is based on their composition (the presence of specific markers), subcellular localization (nuclear, cytoplasmic, axonal etc.), cell of origin (germ cells, neurons), response to stimuli (stress, viral infections), dynamic behaviour and proposed functions (sites of mRNA storage/decay, stress response etc.) (Anderson and Kedersha, 2008).

Besides mRNA, SGs comprise mRNA-bound 48S pre-initiation complexes composed of small ribosomal subunits and translation initiation factors. Moreover, SGs contain proteins involved in mRNA stabilization, processing and transport, such as PABP-1, T cell internal antigen-1 (TIA-1), TIA-1-related (TIAR) and Ras-GTPase-activating protein SH3-domain-binding protein (G3BP1). These proteins can promote SG assembly and serve as specific SGs markers because they are only found in SGs, and not in other cytoplasmic mRNP granules, such as P-bodies or transport granules (Bentmann, Haass and Dormann, 2013).

Stress granules interact with P-bodies (PBs) and are likely to exchange mRNPs between them. Interaction of P-bodies and stress granules suggests a cytoplasmic mRNP cycle wherein.

mRNAs also exchange between polysomes, P-bodies and stress granules. Stress granules are dynamic, and the majority of protein and mRNA components possess rapid recovery rates. On the other hand, mRNAs within P-bodies can return to translation (Buchan and Parker, 2013).

PBs and SGs also several features in common: (1) both are cytoplasmic, seemingly amorphous RNA-protein aggregates that are not surrounded by any membrane as determined by electron microscopy, (2) both are induced by stress conditions, (3) growth in size of both SGs and PBs depends on retrograde transport along microtubules, (4) both SGs and PBs are in exchange with polysomes and contain translationally stalled mRNAs that can re-engage in translation, and (5) there is a large number of proteins, which localize to both PBs and SGs (Kedersha, 2015).

1.4 Stress granules assembly and disassembly

Under acute stress conditions, actively-translating polysomes are rapidly disassembled and, simultaneously, SGs are assembled. The signaling pathway is initiated by the phosphorylation of the alpha subunit of eIF2α, at Serine 51. This phosphorylation inhibits the global protein translation, by the depletion of eIF2α-GTP-tRNAiMet ternary complex. The 48S pre-initiation complex, consisting of one 40S small ribosomal subunit, several eIFs and PABP-1, remains bound to the 5′ UTR of the mRNA (Fig. 3). Although the next step (SGs nucleation) is not yet fully understood, it has been suggested that aggregation-prone RNA-binding proteins, such as G3BP1, TIA-1, fragile X mental retardation protein (FMRP) and tristetraprolin, associate with mRNPs and promote their aggregation. After this primary aggregation step, protein–protein interactions and especially mRNA-bound to PABP-1

aggregate to initiate clustering into SGs. It should be noted that SGs do not have all the properties of aggregates typically associated with neurodegenerative diseases because their formation is fully reversible upon recovery from stress and they do not contain the insoluble, fibrous β-sheet-containing aggregates typically found in most neurodegenerative disorders. Besides eIF2α phosphorylation, other post-translational modifications play an important role in regulating SG assembly or the recruitment of RNA-binding proteins to SGs. O-linked N-acetylglucosamine (O-Glc-NAc)-modified proteins accumulate in SGs and the depletion of key enzymes of the glucose to GlcNAc conversion abolishes SG formation, suggesting that O-GlcNAc modifications are important for proper SGs formation (Anderson and Kedersha, 2007; Takbum Ohn, 2008 ; Bentmann, Haass and Dormann, 2013).

When stress has passed, SGs are rapidly disassembled and polysomes are re-formed (Fig. 3). Because 48S pre-initiation complexes are preserved in SGs in an assembled state, translation can be rapidly reactivated upon stress recovery. The re-formation of polysomes from SGs requires chaperones and can be promoted by the overexpression of staufen or HSP 70. Moreover, this step is regulated by the dual specificity tyrosine-phosphorylation-regulated kinase 3 (DYRK3), which cycles between SGs and the cytosol and regulates SG assembly/disassembly. When DYRK3 kinase activity is inhibited, DYRK3 remains associated with SGs and prevents their dissolution and the release of sequestered mTORC1. When stress signals are gone, the kinase activity of DYRK3 is required for disassembly of SGs and reactivation of mTORC1 signaling (Kedersha *et al.*, 1999 ; Gilks *et al.*, 2004; Bentmann, Haass and Dormann, 2013).

SGs are not stable repositories of untranslated mRNA, as drugs that stabilize (e.g., cycloheximide) or destabilize (e.g., puromycin) polysomes inhibit or promote SG assembly, respectively, which is indicative of a dynamic equilibrium between these structures (Kedersha *et al.*, 2000).

1.4.1 PERKi

Protein kinase R (PKR)-like ER kinase (PERK) is one of three primary effectors of the unfolded protein response, which has a demonstrated role in tumor growth and angiogenesis. PERK is a type I ER membrane protein containing a stress-sensing domain facing the ER lumen, a transmembrane segment, and a cytosolic kinase domain. Upon activation, PERK phosphorylates eIF2α, rendering it an inhibitor of the ribosome translation initiation complex. A potent and selective PERK inhibitor (PERKi) decreases the phosphorylation of eIF2α and consequently reduces the SGs formation (Axten *et al.*, 2012).

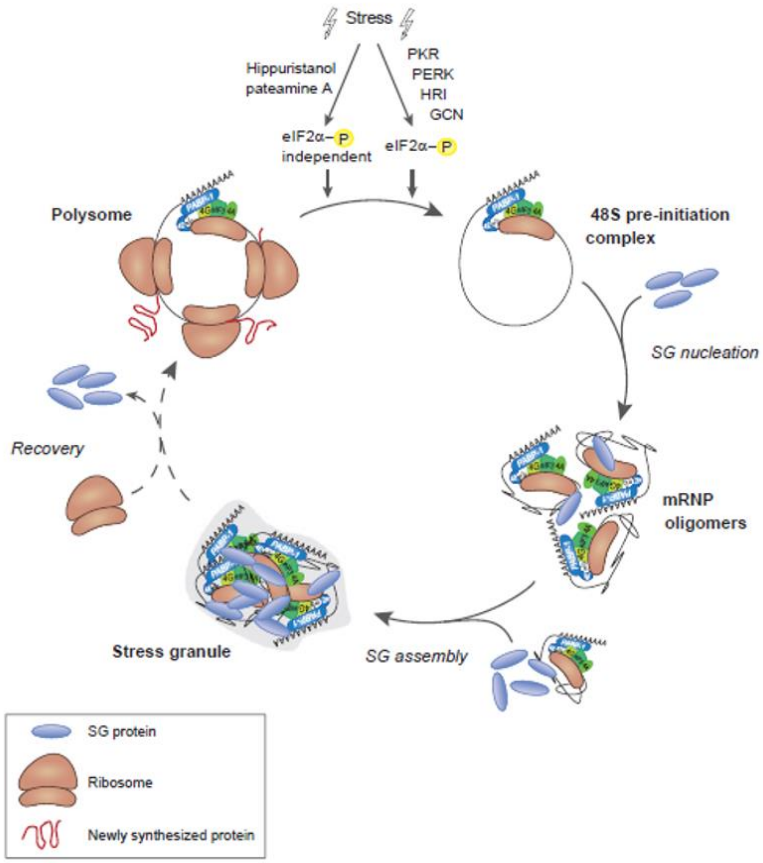

Figure 3 - SGs life cycle. Under physiological conditions, several ribosomes that translate mRNA into protein are bound to an mRNA molecule, forming a polysome. Upon cellular stress, elongating ribosomes run-off the transcript as a result of the reduced availability of eIFs, leaving the 48S pre-initiation complex. SG nucleation is initiated by the recruitment of SG-associated proteins, such as TIA-1, G3BP1 and tristetraprolin, which triggers the aggregation of mRNPs. Subsequently, protein–protein interactions and cross-linking via PABP-1, as well as O-glycosylation of the small ribosomal subunit, facilitate the assembly of the aggregated mRNPs into SGs. During recovery from stress, SG proteins dissociate from the SG, allowing ribosomes to bind and re-form a translating polysome (adapted from Bentmann, Haass and Dormann, 2013).

1.5 Stress granules components

SG components include a diverse group of mRNAs and proteins, some with no previously known links to RNA metabolism (Table 1). The first and defining class of SGs components consists of stalled initiation complexes, still bound to mRNA and recruited to SGs from disassembling polysomes. This class includes mRNA transcripts, eIF3, eIF4F (comprising eIF4E, eIF4A and eIF4G), eIF4B, small ribosomal subunits and PABP-1 (Anderson and Kedersha, 2002). These core SGs components are universal markers for all SGs.

A second class of SG components consists of RNA binding proteins (RBPs) linked to translational silencing or mRNA stability, which are reliable SGs markers but might not be universal to all SGs. Translational silencing members of this group include TIA-1 and TIAR (TIA-1-related), fragile X mental retardation protein (FMRP) and fragile X mental

retardation-related protein 1 (FXR1), FAST, Argonaute and ataxin-2. RNA decay-associated SG components include the Argonaute proteins, tristetraprolin (TTP) and BRF1. Some of these proteins have been observed in polysomes. The latter are probably constitutively active translational silencers: when associated with an mRNA, translation is suppressed and SG assembly is promoted. By contrast, translational silencing must be under regulatory control because they associate with actively translating polysomes (Kedersha *et al.*, 1999; Anderson and Kedersha, 2007).

Table 1 - Selected identified SG-associated proteins (adapated from Anderson and Kedersha, 2007)**.**

Protein	Relevant binding partners	Know function
Ago2	FXR1, RISC	RNAi slicer
Ataxin-2	PABP-1	Translation
Caprin-1	G3BP1	Cell growth
eIF3	40S, eIF4G	Translation
eIF4E	CPEB, smaug, eIF4G,4ET	Translation
eIF4G	eIF4E, eIF3, PABP-1	Translation
FAST	TIA-1	Translation
FBP and KSRP	TIA-1	RNA decay
FMRP and FXR1	Ago2, RISC	Translation
G3BP1	Caprin	Ras signalling
MLNS1	Exon junction	Splicing
PABP-1	eIF4G, eIF3, ataxin-2	Translation, Stability
Plakophilin	G3BP1, FXR1	Adhesion
SRC3	TIA-1	Transcription
SMN	SMN complex	RNP assembly
TIA-1 and TIAR	FAST, SRC3, PMR1, FBP	mRNA silencing
TRAF2	eIF4G	Signalling
TTP and BRF-1	RCK(p54)	mRNA decay

A third class of SGs-associated proteins includes RBPs that regulate aspects of RNA metabolism other than mRNA translation or decay (e.g. splicing, RNA editing and RNA localization). When overexpressed, many of these proteins nucleate SG assembly: G3BP1 (Ras-GTPase-activating protein SH3-domain-binding protein), caprin, FAST, SMN (survival of motor neurons). Some SGs-associated proteins probably serve as molecular scaffolds that define the SGs domain, which remains relatively constant, despite the fact that most SGs proteins thus far examined (e.g. TIA-1, TIAR, G3BP, PABP-1 and TTP) shuttle through SGs much more rapidly than changes in SG morphology would suggest (Kedersha *et al.*, 2000, 2005; Anderson and Kedersha, 2007).

1.6 Stress granules functions

Stress granules have been hypothesized to function in translational repression, given that numerous SGs components are translational repressors, and their formation correlates with decreased global translation (Anderson and Kedersha, 2009). Some specific mRNAs are inefficiently repressed when RBPs that contribute to SGs formation are altered (Mazroui *et al.*, 2007; Tsai, Ho and Wei, 2008), but these effects may simply reflect loss of a specific mRNP regulatory component rather than failure to assemble a granule *per se*. Thus, at the current time, the available evidence suggests that the majority of the translation status of an mRNA is determined by its specific mRNP, and not by its aggregation into stress granules.

Stress granules have also been proposed to function in mRNAs stabilization. During a wide variety of stress responses, mRNA deadenylation, which is a prerequisite for most mRNA degradation, is broadly inhibited (Gowrishankar *et al.*, 2006; Hilgers, Teixeira and Parker, 2006). Moreover, deadenylation is inhibited during stress even when the mRNA is trapped in polysome. SGs are not required for the global stabilization of mRNAs that occur during stress (Hilgers, Teixeira and Parker, 2006).

The formation of SGS will lead to a higher local concentration of their components and a corresponding lower concentration in the remaining cytosol, which has two general effects. First, the concentration of mRNAs and associated proteins into SGs will reduce the concentration of those molecules in the cytosol thereby altering the interactions and rates of biochemical reactions. A second consequence of SGs formation is that the higher local concentration of components in SGs is likely to increase the rates of mRNP assembly or remodelling driven by these factors. This raises the possibility that SGs form to promote assembly of translation initiation complexes by increasing the local concentration of mRNAs

and translation factors, though translation itself is unlikely to occur in SGs given the absence of 60S subunits, and mRNA species which are translated during stress (Kedersha and Anderson, 2002). Assembly of initiation complexes may be especially important during stress when certain translational resources are limiting. Additionally, concentration of various mRNP regulators may also be important in promoting the translation of specific mRNAs that are preferentially translated during stress (Buchan and Parker, 2013).

Thus, SGs are considered to be storage/sorting stations, where transcripts can be stored in a translationally silent form, sorted for translation re-entry or degraded in interacting P-bodies. With this triage, cellular anabolic energy is saved because a portion of the already synthesized mRNAs can be translated at a later time-point and they are not no selectively degraded. Additionally, SGs sequester important signalling molecules and thereby enhance cell survival during stress. SGs sequester regulatory apoptotic proteins (e.g. TRAF2 and RACK1) and thereby inhibit apoptosis. Moreover, the mammalian target of rapamycin complex 1 (mTORC1), a central regulator of cell growth and metabolism, is sequestered into SGs upon cellular stress, which protects cells from DNA damage (Arimoto *et al.*, 2008; Bentmann, Haass and Dormann, 2013; Wippich *et al.*, 2013).

1.7 Stress granules and autophagy

There are two pathways of autophagy and these are mediated by the autophagy-related genes and their associated enzymes: macroautophagy (or autophagy) and microautophagy.

Autophagy is a well-studied system for disposal of a variety of intracellular species. It involves an autophagosome; a double-membrane bound structure that forms from extant membrane-bound organelles. The autophagosome engulfs regions of the cytosol and fuses with the lysosome to become the autophagolysosome where its contents are catabolized. Not all autophagy processes employ the formation of a new autophagosome. Chaperone-mediated autophagy involves the direct targeting of substrates to the lysosome via chaperone intermediates and then active translocation of the substrates across the lysosomal membrane. Microautophagy involves the direct engulfment of cytoplasmic content by invagination of the lysosomal membrane (Chan and Tang, 2013; Gomes and Scorrano, 2013; Monahan, Shewmaker and Bhan, 2016).

The general model of selective autophagic engulfment of substrate is shown in Fig. 4. First, the phospholipid-conjugated LC3 protein facilitates the formation of membranous phagophore structures that recognize the targeted material through various acceptor and

receptor proteins. The phagophore envelops the substrate to form an autophagosome that fuses with the lysosome, forming the autophagolysosome. This structure hosts proteolysis, facilitating amino acid export to the cytosol. Proteins p62 and NBR1 function as selective cargo receptors, linking ubiquitin tags with autophagosome receptors (Klionsky, Eskelinen and Deretic, 2014; Monahan, Shewmaker and Bhan, 2016).

Protein aggregates and RNP granules needed to be disassembled, because large protein aggregates and persistent RNP granules are known to be resistant to ubiquitin-proteasome degradation (Monahan, Shewmaker and Bhan, 2016).

Autophagy is involved in the clearance of RNP granules. Buchan and colleagues demonstrated that SGs breakdown in particular was dependent on selective autophagy (Buchan *et al.*, 2013).

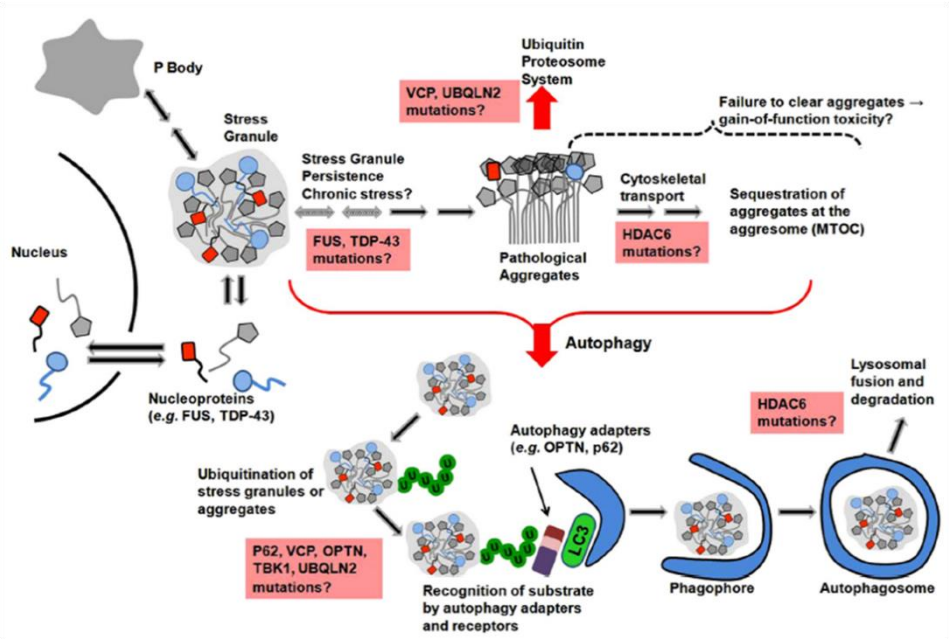

Figure 4 - Schematic showing the connection between stress granules, protein aggregation and autophagy. Boxes in pink indicate mutant genes that could be affecting the indicated process (adapted from Monahan, Shewmaker and Bhan, 2016).

1.8 Stress granules and disease

The formation of SGs is one cellular manifestation in response to stress, which is also connected to the pathogenesis of different human diseases as: neurodegenerative disorders, cancer, virus infections, diabetes and aging. These connections are particularly interesting for health research, as the targeting of SGs may provide new avenues for therapeutic intervention.

The accumulation of insoluble protein aggregates is one of the earliest indicators of cellular stress; and it is also a feature of many neurodegenerative disorders. For example, neurons affected by spinocerebellar ataxia (SCA), Huntington's disease and amyotrophic lateral sclerosis (ALS) contain cytoplasmic SGs and SG-like granules (Bentmann, Haass and Dormann, 2013; Li *et al.*, 2013).

Many cancer cell lines and growing tumours display nucleolar hypertrophy and contain SGs. Notably, SG assembly is also promoted by the chemotherapeutic agents bortezomib and 5-fluorouracil (5-FU). Bortezomib, a FDA-approved anticancer drug that inhibits the proteasome, stimulates SG formation in lung and colon cancer cells. Through the inhibition of rRNA processing in the nucleolus, 5-FU also interferes with ribosome production. Similar to drug treatment, radiotherapy alters nucleolar organization and function, whereas SG assembly can confer resistance to radiotherapy. These observations emphasize the advantage of cancer therapy that reduces nucleolar activities while preventing SGs formation (Moeller *et al.*, 2004; Hein *et al.*, 2013; Mahboubi and Stochaj, 2014).

Diabetic nephropathy, a common complication of type 1 and type 2 diabetes, is linked to nucleoli and granule formation in the cytoplasm. Hyperglycemia can cause kidney cell hypertrophy through the increased production of ribosomes, and SGs are present in the diseased tissue of the diabetic kidney. Senescence modulates the protein profile of nucleoli. It also alters the ability of cells to adapt to a changing environment. When compared to their non-senescent counterparts, some senescent cells generate more SGs, but disassemble SGs at a slower rate. Collectively, these data support the idea that diabetes, certain diabetic complications and aging affect the biology of nucleoli and SGs (Goodman and Building, 2009; Merchant *et al.*, 2009; Liu, Zhou and Lam, 2011; Mariappan *et al.*, 2011).

1.9 Stress granules and neurodegeneration

The potential importance of SGs for neurodegenerative disease becomes apparent because the process of SG formation presents a biological pathway that could be vulnerable to the protein aggregates that accumulate in neurodegenerative disease (Wolozin, 2012; Bentmann, Haass and Dormann, 2013; Wolozin, 2014).

Mutations in RNA binding proteins such as Tar DNA binding protein-43 (TDP-43), Fused in sarcoma (FUS), survival of motor neuron (SMN1), ataxin-2, optineurin (OPT) and angiogenenin (ANG) all cause motor neuron diseases. These proteins could co-localize with

classic SG markers (TIA-1, TIAR and/or G3BP1) in cells undergoing stress (Emde and Hornstein, 2014; Wolozin, 2014).

These RNA binding proteins generally contain two types of conserved domains: glycine rich domains and RNA recognition motifs (RRM). The glycine rich domain is hydrophobic and mediates the reversible aggregation of these proteins; for some RNA binding proteins, such as TIA-1, but not TDP-43. The RRMs have broad specificity, but differ in the spectrum of transcripts bound. For instance, T-intracellular antigen-1 (TIA-1) recognizes transcripts with an uracyl-rich motif with a 30–37 nucleotide long bipartite motif. TIA1 cytotoxic granule-associated RNA binding protein-like 1 (TIAR) binds transcripts with a 28–32 nucleotide long stem loop element (Wolozin, 2012).

Binding of RBPs creates a large macro-molecular complex (Fig. 5) because these proteins contain domains that have low sequence complexity, a high content of glycines, and a strong ability to aggregate. In the core group of nucleating RBPs, appears TIA-1, TIAR and G3BP1, which are thought to initiate formation of the stress granule (Wolozin, 2014).

TDP-43 was discovered to be the major protein that aggregates to form inclusions in amyotrophic lateral sclerosis (ALS) and in frontotemporal dementia (FTLD). When the TDP-43 levels elevates the tendency to aggregate and forming stress granules increase (Hasegawa *et al.*, 2008). It was demonstrated that the TDP-43 pathology occurring in ALS and FTLD co-localizes with other SGs markers (Liu-Yesucevitz *et al.*, 2010).

Inclusions containing FUS, huntingtin, and PrP have all been shown to co-localize with SGs markers (Bosco *et al.*, 2010). It was also demonstrated, that brains of patients with Alzheimer's disease (AD) show large amounts of SGs formation. Interestingly, the SGs proteins that accumulate in AD generally co-localize with tau pathology, and induction of SGs in cells over-expressing tau and TIA-1 appears to be able to induce tau pathology (Vanderweyde *et al.*, 2012).

Others mutated proteins associated with degenerative disease are autophagy-promoting factors (VCP, optineurin, p62, ubiquilin-2142), which is notable given that SGs are cleared via autophagy, and cellular autophagy dysfunction is commonly observed in degenerative disease (Buchan, 2014).

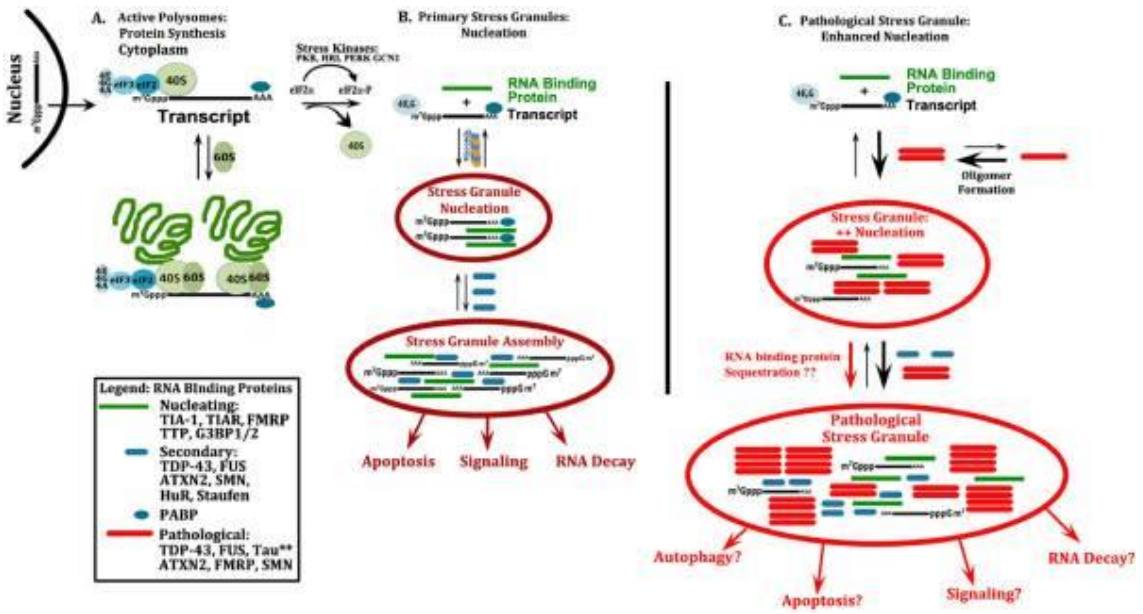

Figure 5 - Mechanism of normal and pathological stress granule formation. A) Normal physiological conditions, neurons synthesize specialized proteins from capped transcripts. B) Stress leads to phosphorylation of eIF2α, dissociation of ribosomes and many of the translation initiation factors, leaving mRNA bound eIF4G and poly-A binding protein. Nucleating RNA binding proteins bind the free RNA and also form protein/protein complexes, which initiate stress granule formation. C) Pathological proteins, such as TDP-43, FUS and tau, have a strong tendency to form oligomers, and then fibrils. The consolidation of RNA binding proteins during SG formation might promote oligomerization by creating cellular domains with higher concentrations of these proteins (adapted from Wolozin, 2012).

1.10 Polyglutamine disorders

Polyglutamine disorders consist in a group of neurodegenerative diseases: HD, DRPLA, SBMA, and six forms of spinocerebellar ataxias (Table 2). All disorders are progressive, typically striking in midlife and causing increasing neuronal dysfunction and in some cases neuronal loss, 10 to 20 years after onset of symptoms, allowing the wide range of neurological, psychiatric and motor symptoms present (Zoghbi and Orr, 2000; Orr and Zoghbi, 2007).

An important common feature to all Polyglutamine disorders is the negative correlation between the age of onset and the number of CAG repeats, leading to an earlier development of the disease. The genetic similarities among all these diseases could indicate a possible common mechanism of pathogenesis, caused by the toxic properties. The expanded Polyglutamine tract within a target protein facilitates transition to a novel and toxic conformation, causing alterations. Toxicity may be caused by the peptide as a monomer or it associated form - oligomers. The oligomers can assemble into a larger aggregated species and eventually are deposited in intracellular inclusions. The main toxic effects of the pathological protein include transcriptional changes, caused by interactions of the expanded

protein with transcriptional factors. One example is the proteotoxic stress as a result of the disruption of the quality control systems of the cell and metabolism and mitochondrial dysfunction (Gatchel and Zoghbi, 2005; Shao and Diamond, 2007; O. Riess, 2008).

Table 2 - Molecular characteristics of Polyglutamine neurodegenerative diseases (adapted from Zoghbi and Orr, 2000).

Poly Q Diseases	Locus	Protein	Normal CAG expansion repeats	Pathological CAG expansion repeats	Localization of inclusions	Affected brain regions
DRPLA	12q	Atrophin-1	6-35	49-88	Nuclear	Cerebellum, central cortex, basal ganglia, Luys body
HD	4q16.3	Huntingtin	6-35	36-121	Nuclear and cytoplasmatic	Striatum and cerebral cortex
SBMA	Xq11-12	Androgen receptor	9-36	38-62	Nuclear and cytoplasmatic	Anterior horn and bulbar neurons, dorsal root ganglia
SCA1	6p22-23	Ataxin-1	6-44	39-82	Nuclear	Cerebellar Purkinje cells, dentate nucleus, brainstem
SCA2	12q23-24	Ataxin-2	15-31	36-63	Nuclear and cytoplasmatic	Cerebellar Purkinje cells, brainstem, frontotemporal lobes
SCA3/MJD	14q24.3-31	Ataxin-3	10-51	55-84	Nuclear	Cerebellar dentate neurons, basal ganglia, brain stem, spinal cord
SCA6	19p13	CACNAIA	4-18	21-33	Cytoplasmatic	Cerebellar Purkinje cells, dentate nucleus, inferior olive
SCA7	3p12-p21.1	Ataxin-7	4-35	37-306	Nuclear	Cerebellum, brain stem, macula, visual cortex
SCA17	6q27	TBBP	25-42	47-63	Nuclear	Cerebellar Purkinje cells, inferior olive

DRPLA: Dentarubral-pallidoluysian atrophy; **HD**: Huntington's disease; **SBMA**: Spinal and bulbar muscular atrophy; **SCA1**: Spinocerebellar ataxia type 1; **SCA2**: Spinocerebellar ataxia type 2; **SCA3/MJD**: Spinocerebellar ataxia type 3/ Machado Joseph Disease; **SCA6**: Spinocerebellar ataxia type 6; **SCA7**: Spinocerebellar ataxia type 7; **SCA17**: Spinocerebellar ataxia type 17.

Spinocerebellar ataxia type 2 (SCA2) and Spinocerebellar ataxia type 3 (SCA3) are the most prevalent dominant ataxias. They are caused by a trinucleotide expansion in the SCA2 and MJD1 genes, respectively. These mutated genes encode for a expandend Polyglutamine stretch in the gene product ataxin-2 for SCA2, and ataxin-3 for SCA3/MJD.

1.10.1 SCA3/MJD

Machado-Joseph disease, also known as Spinocerebellar ataxia type 3, is the most common inherited spinocerebellar ataxia worldwide. In MJD, a CAG repeat expansion encodes an abnormally long polyglutamine tract in the disease protein, ataxin-3. MJD was first described in Northern American families of Azorean ancestry. The wild-type (WT) alleles of MJD range from 10 to 51 CAG repeats, whereas MJD patients alleles range from 52 up to 87 repeats (Paulson, 2013).

Cerebellar ataxia, progressive external ophthalmoplegia, dysarthria, dysphagia, pyramidal signs, dystonia, rigidity, and distal muscle atrophies are some of the symptoms displayed by MJD patients (Paulson, 2007; Pastore, Bauer and Scho, 2008).

Neuroimaging studies have revealed atrophy of the pons, cerebellar vermis and hemispheres, basal ganglia (globus pallidus, caudate and putamen), midbrain and medulla oblongata. The atrophy in the cerebellum and brainstem is progressive and dependent on the length of the CAG repeat and the age of the patients (Hans-Juergen Machulla, 2005; Eichler *et al.*, 2011).

Ataxin-3 is a small, soluble protein that can shuttle in and out of the nucleus. In many cells a fraction of the cellular pool of ataxin-3 is intranuclear, bound to the nuclear matrix. In unaffected brain and in normal neurons, ataxin-3 appears to be largely cytoplasmic. In disease brain, however, the protein tends to concentrate in neuronal cell nuclei. Because ataxin-3 orthologs in other vertebrates have a much smaller polyglutamine domain, a large glutamine repeat is clearly not essential for the core functions of ataxin-3. Ataxin-3 orthologs, however, share an evolutionarily conserved, N-terminal Josephin domain. In addition to its Josephin and polyglutamine domains, ataxin-3 has a predicted coiled-coil domain, two closely spaced ubiquitin interacting motifs (UIMs) upstream of the polyglutamine domain and, in one of two major splice variants, a third UIM downstream of the polyglutamine tract. Ataxin-3 can cleave poly-ubiquitin chains from test substrates and poly-ubiquitin chains *in vitro* and, when the active site cysteine residue is mutated, this de-ubiquitinating activity is lost. When expressed in cells, catalytically inactive ataxin-3 causes a build-up of poly-ubiquitinated proteins (Scheel *et al.*, 2003; Winborn *et al.*, 2008; Matilla-dueñas *et al.*, 2012; Paulson, 2013).

1.10.2 SCA2

SCA2 was initially reported by Wadia and Swami in India in the year 1971. These authors described it as a heredodegenerative ataxia characterized by slow saccadic eye velocity and limited ocular movements. The most frequent clinical characteristics include progressive cerebellar syndrome, ataxic gait, cerebellar dysarthria, dysmetria, dysdiadochokinesia associated with slow saccadic movements, peripheral neuropathies, fasciculations, painful muscle contractures, sleep disorders, and dysphagia. The mutation that produces SCA2 consists of an abnormal expansion of the CAG trinucleotide localized in exon 1 of the gene denominated ATXN2, which mapped in the 12q23-24 chromosomal region. Alleles of the ATXN2 gene that carry 13–31 CAG-trinucleotide repeats are present in normal individuals. Alleles with a CAG triplet repeat number of >31 and up to approximately 200 are present in patients with SCA2 (Wadia and Swami, 1971; Velázquez-Pérez *et al.*, 2004, 2007, 2009, 2010; Chou, Koeppe and Bohnen, 2011; Magaña, Velázquez-Pérez and Cisneros, 2013).

Neuropathologic phenotype of SCA2 is characterised by degeneration of the olivopontocerebellar system as well as substantia nigra (SN), striatum and globus pallidus. Volume and weight diminution of the brain stem and loss of Purkinje cells in both hemispheres (Pang *et al.*, 2002; Takao *et al.*, 2011).

Ataxin-2 is a 140 kDa protein (1,312 amino acid residues) that exhibits no sequence similarity with other polyglutamine-rich proteins associated with neurological diseases, with the exception of the glutamine-rich domain, which increases its molecular mass according to the length of the CAG-repeat expansion (Albrecht *et al.*, 2004). It possesses two important domains:

(1) The Like Sm domain (Lsm domain) and the Lsm-associated domain. It also presents one region localized next to the carboxyl-terminal region, which are denominated PABPC1-interacting motif-2 (PAM2) (Satterfield and Pallanck, 2006; Loo, van de *et al.*, 2009).

(2) Ataxin-2 Lsm domain is shared with proteins involved in RNA posttranscriptional modifications (Pulst, 2003). PAM2 domain participates in RNA-messenger stability and translation regulation, because interacts with the PAB6 domain of the PABP (Ralser *et al.*, 2005). The ataxin-2 carboxyl-terminal region, its interaction with an ataxin-2-binding protein (A2BP1). A2BP1 contains a ribonucleoprotein motif, characteristic of RBPs, and regulates the RNA splicing (Lee, Tang and Black, 2009).

Association of ataxin-2 with the endoplasmic reticulum and its participation in the formation of SGs suggest that this protein could interact with the plasma membrane, performing some

particular function. It has been reported that ataxin-2 interacts with endophilins A1 and A3, proteins that are implicated in the formation of plasmatic membrane curvature at endocytotic sites, through the activation of an ubiquitination-regulated protein complex coupled with actin filaments (Swisher and Parker, 2010).

In SCA2-transgenic mouse denominated Q58 (mutant ataxin-2), ataxin-2 interacts with the carboxyl-terminal region of the type 1 inositol (1,4,5)-triphosphate (receptor of the calcium channel), affecting the intracellular signalling pathway, which leads to an increase of glutamate and apoptosis in neuronal cells. Suggesting its participation in calcium-mediated cell-signalling cascades (Huynh *et al.*, 2000).

As ataxin-2 is a cytoplasmic protein with higher expression in Purkinje cells, the mutant ataxin- 2 presents abnormal folding that gives rise to the formation of aggregates, which might trigger a series of events that lead to programmed cell death and consequently to the degeneration of central and peripheral neuronal structures. Ubiquitinated intranuclear inclusions are found in neurons of SCA2 patients but not in the Purkinje cells. Interestingly, recruitment of ataxin-1, ataxin-3, and TATA box-binding protein was found in neuronal intranuclear inclusions in SCA1, SCA2, and SCA3 human brains, raising the possibility that nuclear aggregates alter the transcriptional process. It is thought that cytoplasmic and nuclear aggregation of ataxin-2 is involved in SCA2 pathology; however, this issue is controversial, because aggregation may merely represent end products of the upstream toxic events. In fact, several cell and animal models for polyglutamine disorders show the discrepancy between inclusion formation and cell death (Koyano *et al.*, 1999; Uchihara *et al.*, 2001; Huynh *et al.*, 2003; Neurochemistry, 2009; Magaña, Velázquez-Pérez and Cisneros, 2013).

Ataxin-2 suffers different posttranslational modifications including proteolytic cleavage, phosphorylation, and ubiquitination, which might alter the characteristics and consequently the function of both wildtype and mutant variants (Koyano *et al.*, 1999; Turnbull *et al.*, 2004).

SGs harbour a wide variety or RBPs, and could be involved in disease, such as ataxin-2, FUS and TDP-43. When occurs mutations in these proteins cause SCA2 (ataxin-2) and ALS (FUS and TDP-43). Mutations in RBPs increase propensity to aggregate and to form SGs either by directly increasing the tendency of the protein to aggregate, or by preventing nuclear translocation. They have a strong tendency to form oligomers, and then fibrils. The consolidation of RBPs during SGs formation might promote oligomerization by creating cellular domains with higher concentrations of these proteins. The increased stability of

oligomers and fibrils might serve as a nidus for SG formation, leading to SGs formation (Wolozin, 2012; Li et al., 2013; Wolozin, 2014).

Different mutations in ataxin 2 (long and intermediate length polyQ expansions) could contribute to distinct phenotypic consequences in ALS, but also in SCA2. One potential explanation is that intermediate-length polyQ expansions in ataxin 2 result in enhanced stress-induced caspase activation, which leads to increased TDP-43 pathological modifications, including cleavage and hyperphosphorylation (Fig. 6) (Ding *et al.*, 2013).

PolyQ expansions in ataxin 2 could contribute to disease by hampering the ability of SGs to dissolve properly (Fig. 6).

Ataxin 2 and SGs, with their roles in sensing and responding to environmental stresses, might help to explain the connection between environmental exposures, including traumatic injury, and the pathogenesis of disease and in particular neurodegenerative disorders. Upon exposure to stress, RBPs move from the nucleus to the cytoplasm and associate with ataxin-2 containing SGs. Once the stress subsides, SGs no longer aggregate, and the RBPs translocate back to the nucleus. This repeated cycle of aggregation and disaggregation, over the course of a lifetime, perhaps more so when exposed to specific environmental exposures and traumas, can become misregulated and can lead to the improper cytoplasmic localization of one or more of these proteins. This failure to restore nuclear localization of these proteins could cause the subsequent disease pathology (Fig. 6). Age-dependent breakdown in cellular proteostasis may lead to further defects in maintaining SGs protein quality control and likely underpins the late-onset aspect of disease (Bosco *et al.*, 2010; Dormann *et al.*, 2010; Liu-Yesucevitz *et al.*, 2010; Li *et al.*, 2013) .

Intermediate-length ataxin 2 polyQ expansions (27–33 Qs), longer than normal but not past the threshold for SCA2, were recently associated with increased risk for ALS (Elden *et al.*, 2011).

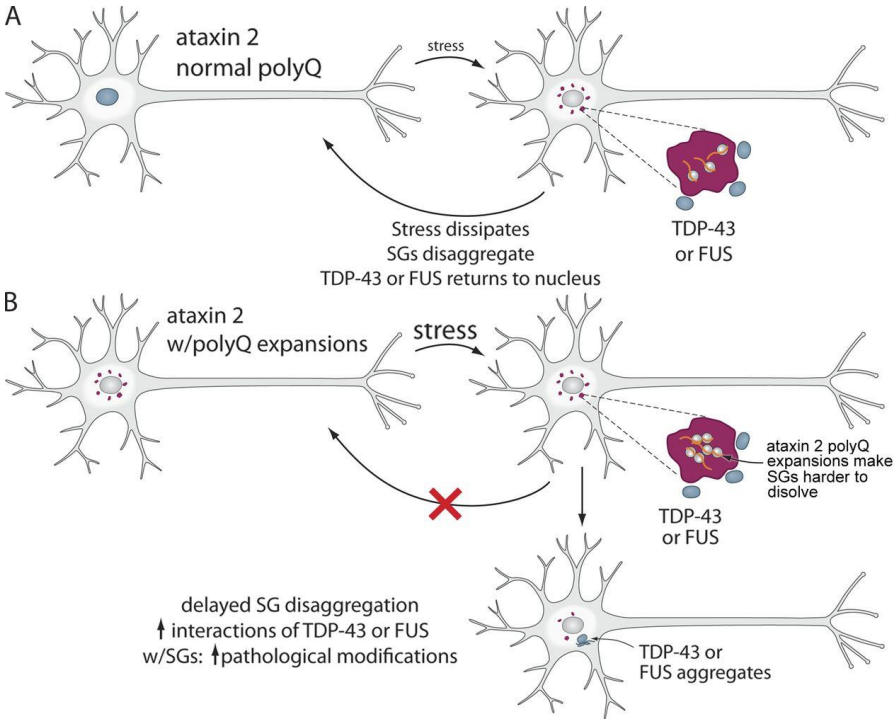

Figure 6 - How ataxin 2 polyQ expansions might affect SGs. A) SGs form upon cellular stress. The ataxin 2 polyQ length is normally 22 Q. When the stress dissipates, SGs dissolve. (B) In the presence of a pathogenic ataxin 2 polyQ expansion, the SGs might be more difficult to dissolve, perhaps owing to increased ataxin 2 stability (adapted from Li *et al.*, 2013).

Objectives

The main objective of this work was shed some understanding in the possible role of stress granules (SGs) in neurodegenerative diseases, particularly in SCA2 and SCA3 diseases. More specifically we wanted to study how the SGs inhibition could influence ataxin-2 or ataxin-3 proteins, using a pharmacological approach (PERK inhibitor, GSK2606414), or a molecular approach (RNAi silencing through shRNAs). The idea behind the study was to hypothesize that PERK inhibiton, which decreases eIF2alpha phosphorylation might provide a new therapeutic intervention for these diseases.

The specific objectives were:

- To evaluate the levels of eIF2alpha/Phospho-eIF2alpha, ataxin 2 and ataxin 3 in SCA2/SCA3 models;
- To evaluate the PERK inhibitor toxicity (*in vitro*);
- To evaluate how the PERK inhibitor affects the levels of ataxin-2 and ataxin-3;
- To investigate how the stress granules stimulus removal affects the levels of ataxin-2 and ataxin-3;
- To evaluate how the eIF2alpha phosphorylation inhibition impacts the aggregation of ataxin-2 and ataxin-3:
    - In SCA2/SCA3 cell models (PERKi and shPERK);
    - In SCA3 animal models (shPERK).

CHAPTER II – MATERIALS AND METHODS

2.1 *In vitro* Experiments

2.1.1 Neuroblastoma Cell Culture

Mouse neuroblastoma cell line (Neuro-2A cells) obtained from the American Type Culture Collection cell biology bank (CCL-131) were incubated in Dulbecco's modified Eagle's medium supplemented (DMEM) with 10% fetal bovine serum (FBS), 100U/mL penicillin and 100mg/mL streptomycin (Gibco) (complete medium) at 37°C in 5% CO_2/air atmosphere.

2.1.2 Neuroblastoma Cell Transfection

200.000 Neuro2A cells were plated per well into 12 multi-well plates and transfected with plasmids of interest 24 hours after plating: 1ug of each plasmid of interest per well. PEI 'Max' (Polyehtylenimine) was used to transfect the cells, which forms precipitates with the DNA. For this, PEI 'Max' was pipetted into non-supplemented DMEM along with the DNAs of interest. After 10 minutes, PEI was inhibited with supplemented DMEM and this mixture was plated in the multi-wells. The multi-wells were incubated at 37°C in 5% CO_2/air for 48h.

2.1.3 PERKi treatment

Neuro-2A cells were plated and 24h after were treated with crescent concentrations of PERKi at different times of treatment. GSK2606414 (PERK inhibitor; EMD Millipore, 516535) was added directly to medium from a 1mg/mL stock diluted in DMSO, at concentrations: 100nM, 200nM, 500nM, 1μM, for 24h and 48h. Upon choosing the ideal concentration and time point, the procedure was repeated only with the defined set: 200nM at 48h.

2.1.4 Stress Granules induction

Neuro-2A cells were plated and 24h after were transfected with the plasmids of interest and treated with the PERKi. 48h after transfection stress granules were induced; 10μL was added directly to medium from a 100mg/mL stock of sodium arsenite (SA, Sigma Aldrich 10μL/mL to a final 0,05M concentration). The stimulus was maintained for 1h and then cells were collected for posterior analysis.

2.1.5 Cell viability assay / ALAMAR assay

Cell viability under the different experimental conditions was assessed by a modified alamarBlue® assay. At several time-points after transfection or infection, the cells were incubated with Dulbecco's modified Eagle medium containing 10% (v/v) alamarBlue® dye. After a 1h incubation period at 37°C, the absorbance of the medium was measured at 570nm and 600nm. Cell viability was calculated as a percentage of the control cells (non-transfected/infected), according to:

Cell viability (% of control) = $[(A_{570} - A_{600})$ of treated cells $\times$ 100/$(A_{570} - A_{600})$ of control cells].

2.1.6 Puromycin translation rate assay

Neuro2A cells were plated and 24h after were incubated with sodium arsenite (1mg/mL), PERKi (200nM) and shPERK (500ng). At 48 hours post-plating puromycin (10µg/ml) was added to all conditions for 45 minutes. Ciclohexamide (CHX, 10µg) was used as a positive control and a well of non-treated cells as a negative control. Cells were collected and global protein synthesis was measured by Western Blot.

2.1.7 Protein Extraction and Western Blot

Collected cells from the different experiments were lysed on ice in RIPA (radio-immunoprecipitation assay) buffer [50 mM Tris·HCl, pH 7.4; 150mM NaCl; 5mM EDTA; 1% Triton X-100; 0.5% deoxycholate; 0.1% SDS; 200µM phenylmethylsulphonylfluoride; 1mM DTT, 1mM Na3VO4; 10mM NaF], supplemented with mini protease inhibitor mixture tablet (Roche) and also phosphatase inhibitor tablet (PhosphoStop, Roche). Lysates were incubated for 15min at 4°C, and the insoluble material was pelleted by centrifugation for 10min at 16,000 × g and 4°C. The protein concentration of each sample was determined by the bicinchoninic acid protein assay (PierceTM BCA Protein Assay Kit; Thermo). The samples were denaturalized by adding 6X concentrated sample buffer [0.5M Tris, 30% (vol/vol) glycerol, 10% (wt/vol) SDS, 0.6M DTT, 0.012% bromophenol blue] and heating for 5min at 95°C. Samples were stored at −20°C until use. Equal amounts of total protein were loaded per lane and separated by electrophoresis in 4–10% (wt/vol) (4% stacking and 10% running) SDS polyacrylamide gels (SDS/PAGE). Proteins were then transferred electrophoretically in CAPS buffer [0.1M CAPS, pH 11; 10% (vol/vol) methanol] to polyvinylidenedi fluoride (PVDF) membranes (Millipore). The membranes were blocked with 5% (wt/vol) low-fat milk

in Tris-buffered saline (137mM NaCl, 20mM Tris·HCl, pH 7.6) containing 0.1% Tween 20 (TBS-T) for 1h at room temperature. The membranes were incubated overnight with the primary antibodies at 4°C. The primary antibodies used were as follows: mouse anti-Atxn2 (1:1000; BD Biosciences), mouse anti-Atxn3 (1H9; 1:5000; Millipore), mouse anti-puromycin (1:20000; Millipore), rabbit anti-eIF2alpha (prepared in BSA 5%; 1:1000; Cell Signalling), rabbit anti-Phospho-eIF2alpha (1:1000; Millipore), rabbit anti-G3BP1 (1:1000; Millipore), rabbit anti-P62 (prepared in BSA 5%; 1:1000; Cell Signaling). After three washes with TBS-T, the membranes were incubated for 1h, at room temperature, followed by the incubation with the corresponding alkaline phosphatase-linked secondary goat anti-mouse (1:10000; Vector Laboratories) or IgG anti-rabbit (1:10000; Vector Laboratories). Protein immunoreactive bands were visualized by chemifluorescence with the ECF substrate (GE Healthcare) in a VersaDoc Imaging System Model 3000 (Bio-Rad). The membranes were reprobed with a monoclonal anti–β-tubulin antibody (1:10,000; Sigma-Aldrich) for equal protein loading control. The optical density of the bands was quantified with the Quantity One Software (Bio-Rad). The results are normalized to β-tubulin and expressed as the relative amount compared with control.

2.1.8 Immunocytochemistry

The immunocytochemical procedure was initiated by fixating cells into glass coverslips with 4% paraformaldehyde fixative solution for 20min, and after washing with 0.1M phosphate buffer solution. Then samples were incubated for 5min with PBS containing 0.25% Triton™ X-100. Blocking was made for 1h in PBS with 3% bovine serum albumin (BSA, Sigma). Primary antibody was incubated overnight at 4°C in blocking solution in the proper dilution: rabbit anti-PABP (1:500; Millipore) and rabbit anti-TIA1 (1:500; BD Biosciences), and the secondary antibody (1:200) for 2h at room temperature. The secondary antibody used was coupled to a fluorophore (Alexa Fluor®, Invitrogen) and followed by a nuclei staining reaction with 4',6-diamino-2-phenylindole (DAPI, 5 min, at room temperature). The coverslips were then mounted in FluorSave™ Reagent (Calbiochem) on microscope slides.

2.2 *In vivo* Experiments

2.2.1 Animals

8-week-old C57/BL6 male mice (Charles River) were used in this experiment. The animals were housed in a temperature controlled room maintained on a 12h light/ 12h dark cycle. Food and water were provided *ad libitum*. The experiments were carried out in accordance with the European Community directive (86/609/EEC) for the care and use of laboratory animals.

2.2.2 DNA constructs

Plasmids encoding for mutant ataxin-3 with 84 glutamines (Atxn3MUT (only used *in vitro*) or Atxn3-84Q), full-length wild-type ataxin-3 with 28 glutamines (Atxn3WT (only used *in vitro*) or Atxn3-28Q) (Matos *et al.*, 2016); full-length mutant ataxin-2 with 58 glutamines (Atxn2MUT), full-length wild-type ataxin-2 with 22 glutamines (Atxn2WT) (Huynh *et al.*, 2003); full-length mutant ataxin-3 with 72 glutamines (isoform MJD1a, full-length; Atxn3MUT (only used *in vivo*) or Atxn3-72Q), full-length wild-type ataxin-3 with 27 glutamines (Atxn3WT or Atxn3-27Q) (Alves *et al.*, 2008); shPERK (Mission® shRNA; Sigma-Aldrich; 09111509MN); shGFP (Alves *et al.*, 2008); and GFP under the control of the phosphoglycerate kinase promoter, cloned, and used previously in the context of MJD were produced in HEK293T cells using a four-plasmid system described previously (Almeida, de *et al.*, 2001). The lentiviral particles were produced and resuspended in 0.1 M phosphate-buffered saline (PBS) with 0.5% bovine serum albumin, and samples were matched for particle concentration by measuring HIV-1 p24 antigen content (RETROtek, Gentaur, Belgium). Concentrated viral stocks were stored at −80 °C until use.

2.2.3 Stereotaxic injection in the striatum

Concentrated viral stocks were thawed on ice and resuspended by repeated pipetting. Lentiviral vectors were stereotaxically injected into the right/left hemisphere of the striatum in the following coordinates: antero-posterior: +0.6mm; lateral; -1.8mm (right hemisphere) or +1.8mm (left hemisphere); ventral: -3.3mm; mouth bar: 0. Animals were anesthetized by administration of a mixture of ketamine (100mg/kg, Clorketam 1000, Vétaquinol) with xylazine (10mg/kg, Rompun®, Bayer) by intraperitoneal injection. Particle contents of the viral vectors were determined by p24 antigen ELISA (RETROtek, Gentaur, France) and a

single injection with 400.000ng of viral vectors (2 studies were performed: in the first one 400.000ng/µL of virus was injected in total (toxicity study), in the second one was injected 400.000ng/µL of Atxn3 MUT (mutant Ataxin 3 with 72 glutamines) and 400.000ng/µL of shPERK) were injected at a rate of 0.25µl/min by means of an automatic injector (Stoelting Co., Wood Dale, IL, USA) into the mouse brain area through a 34-gauge blunt-tip needle linked to a Hamilton syringe (Hamilton, Reno, NV, USA). After injection, the syringe needle was left in place for an additional 5min to allow the viral vector diffusion and to minimize backflow. Mice were kept in their home cages for 4 weeks of treatment before being sacrificed.

2.2.4 Tissue preparation

Animals were sacrificed four weeks post injection by sodium pentobarbital overdose, transcardially perfused with 0.1 M phosphate buffer solution and a 4% paraformaldehyde fixative solution (Fluka, Sigma) followed by brain removal. The brains were removed and post-fixed in 4% paraformaldehyde for 24h and cryoprotected by incubation in 20% sucrose/phosphate buffer for 48h. The brain was frozen and sectioned using a cryostat (LEICA CM3050 S). The striatal injections coronal sections of 25µm were made. Slices were collected and stored in 48-well trays, free-floating in 0.1M phosphate buffer solution supplemented with 0.12mmol/L sodium azide. The plates were stored at 4°C until immunohistochemical processing. Samples were kept at −80°C for posterior processing.

2.2.5 Immunohistochemistry

The immunohistochemical procedure for light microscopy was initiated by incubating free-floating sections for 30min at 37°C in PBS containing 0.1% diphenylhydrazine, to inhibit endogenous peroxidases. The sections were incubated at RT for 1h in blocking solution (0.1% Triton X-100 containing 10% Normal Goat Serum (NGS, Gibco) in PBS), and then with the appropriate antibodies: rabbit anti-dopamine and cyclic AMP-regulated neuronal phosphoprotein 32 (DARPP-32) antibody (1:2000; Merck Millipore; overnight at 4°C) diluted in the blocking solution. After overnight incubation three washings were performed and the sections were incubated with the corresponding biotinylated secondary antibody (1:200; Vector Laboratories Inc., CA, USA) diluted in the blocking solution for 2h at RT. After three washes, bound antibodies were visualized by the ABC amplification system (VECTASTAIN® ABC kit, Vector Laboratories, West Grove, USA) and 3,3′- diaminobenzidine

tetrahydrochloride (peroxidase substrate kit, DAB, Vector Laboratories, CA, USA) as the substrate. The sections were mounted, hydrated (with H2O mQ) and then dehydrated by passing through an increased degree of ethanol solutions (ETOH 75%, 96% and 100%) and xylene solution, and cover slipped with Eukitt (O. Kindler GmbH & CO, Freiburg, Germany).

Fluorescence immunohistochemical procedure was also performed. Free floating sections were incubated at RT for 1h in blocking solution (0.1% Triton X-100 containing 10% NGS (Gibco) in PBS), and then in the blocking solution containing the appropriate e antibodies: anti-IBA-1 (1:1000, Wako, overnight at 4°C), anti-GFAP (1:1000, DAKO, overnight at 4°C). After three washes, the sections were incubated with the corresponding secondary antibodies coupled to fluorophores Alexa Fluor 488 or Alexa Fluor 594 (1:250, Molecular Probes-Invitrogen, Eugene, OR) diluted in blocking solution for 2h at RT. The sections were washed three times and incubated during 5min with 4',6'-diamidino-2- phenylindole DAPI (Sigma; St. Louis; MO), washed and mounted in Mowiol on microscope slides. Staining was visualized using Zeiss Axioskop 2 plus, Zeiss Axiovert 200 and Zeiss LSM 510 Meta imaging microscopes (Carl Zeiss Microimaging, Germany), equipped with AxioCam HR color digital cameras (Carl Zeiss Microimaging) using 5x, 20x and 40x Plan-Neofluar objectives and the AxioVision 4.7 software package (Carl Zeiss Microimaging). Quantitative analysis of fluorescence was performed with a semi-automated image-analysis software package (Image J software, USA).

2.2.6 Analysis of the volume of DARPP-32 depletion region

The extent of striatal mutant ataxin-3 72Q lesions was evaluated by photographing, with a x20 objective, 8 sections stained with DARPP-32 per animal (25 µm-thick sections at 200 µm intervals) were selected to obtain rostro-caudal sampling of the striatum. The area of the lesion was quantified with a semi-automated image-analysis software package (ImageJ, NIH, USA). The area of the striatum showing a loss of DARPP-32 staining was measured for each animal, with an operator-independent macro. The volume was then estimated with the following formula: volume = $d(a_1+a_2+\ldots+a_7+a_8)$, where d is the distance between serial sections (200 µm) and a_{1-8} are DARPP-32 depleted areas for individual serial sections. The depleted area corresponds to area with a gray-scale value lower than the mean gray-scale value of all pixels measured in the lesioned area. Data were expressed as the evaluated DARP-32 depleted volume (mm^3).

2.2.7 Cresyl Violet Staining

The striatal sections were hydrated by stained with water for 30 seconds; dehydrated with etanol 96%, etanol 100%, xylene and etanol 75% corresponding, 3min in witch solution; rehydrated in water, 30 seconds; stained in cresyl violet differentiated in acetate buffer pH 3.8 to 4 (2.72% sodium acetate and 1.2% acetic acid; 1:4 v/v), for 5min; rehydrated with water, 30 seconds; and finally dehydrated with etanol 75%, etanol 96%, etanol 100% and xylene corresponding, 3min each. Mounted with Eukitt® (O. Kindler GmbH & CO. Freiburg, Germany).

2.3 Statistical Analysis

Results are expressed as mean ± SEM. Data were analyzed by using one-way analysis of variance (ANOVA), or Student's unpaired *T* test with two-tailed *P* value when comparing two groups only, or Student´s paired *T* test with two-tailed P value when comparing two groups where the values of one column are identical. A value of $P < 0.05$ was considered significant. Prism 5.0 (GraphPad Software) was used for all statistical analysis.

CHAPTER III – RESULTS AND DISCUSSION

3.1 Cell viability is reduced upon crescent concentration of PERKi

Firstly, we wanted to test different concentrations of PERKi (GSK2606414), to find the ideal concentration to use in our studies. So we perform an experiment to evaluate the cell viability at different concentrations (100nM, 200nM, 500nM and 1μM) of the PERKi, using neuro2A cells **(Fig. 7A)**. We observed that the cell viability is reduced upon crescent concentration of PERKi, as recently been described (Kim *et al.*, 2014).

After that, we perform an experience to evaluate the cell viability in neuro2A transfected cells, with the 200nM and 500nM concentrations, and see with the cell viability of the transfected cells was the same of the non-transfected cells. The cells were transfected with ataxin-2 WT (Q22) and ataxin-2 MUT (Q58), and we have chosen the 200nM and the 500nM concentrations because were the two highest concentrations of PERKi well tolerated by the cells. We observed that the transfected cells have the same behavior of the non-transfected cells **(Fig. 7B)**, which is upon crescent concentrations of PERKi the cell viability is reduced.

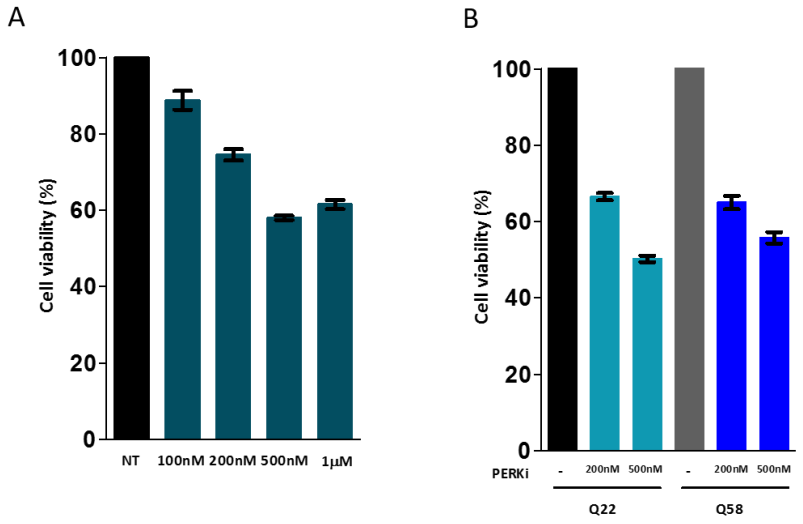

Figure 7 - Cell viability is reduced in higher concentrations of PERKi. (A) Cell viability of non-transfected neuro2A cells, treated with different concentrations of PERKi (100nM, 200nM, 500nM and 1μM). Cell viability assay or ALAMAR assay of non-transfected neuro2A cells show that upon crescent concentrations of PERKi, the cell viability is reduced. **(B)** Cell viability of transfected neuro2A cells (transfected with ataxin-2 WT and ataxin-2 MUT), treated with two different concentrations of PERKi (200nM and 500nM). Once again, the cell viability assay show that in transfected neuro2A cells the cell viability is reduced upon higher concentration of PERKi. **(A-B)** n=4 independent experiments.

Taken together, these data indicate that the 200nM concentration of PERKi is the best and the chosen concentration to use in the posterior experiences: it is the higher concentration of PERKi where the cell viability is well tolerated by the neuro2A cells (>75%).

All of these experiences were performed at 24h and 48h, and the time-point 48h of treatment was the chosen one. The cell viability was more reduced and in previous studies, the authors also show that bigger time-points of PERKi treatment leads to a more effective inhibition of PERK (Kim *et al.*, 2014).

3.2 PERKi treatment reduces the phospho-eIF2alpha levels but shPERK don't

Next we wanted to investigate if the PERKi was effectively inhibiting protein kinase R (PKR)-like endoplasmic reticulum kinase (PERK). This protein is activated in response to a variety of endoplasmic reticulum stresses. Upon activation, PERK phosphorylates eIF2alpha, rendering it an inhibitor of the ribosome translation initiation complex (Axten *et al.*, 2012). To do that, we evaluate the levels of phospho-eIF2alpha and eIF2alpha in neuro2A cells. If the phospho-eIF2alpha levels were reduced, it might suggest that there was an inhibition of the PERK.

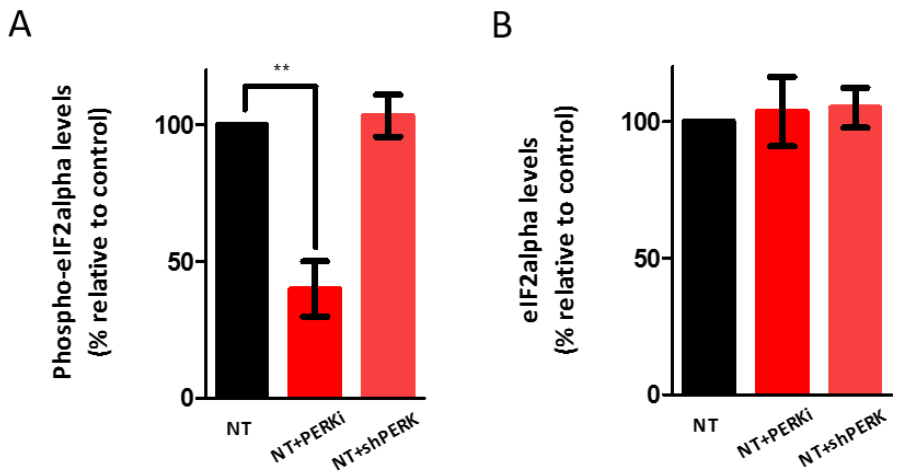

Figure 8 - Phospho-eIF2alpha levels are reduced at the treatment of PERKi but not at the shPERK transfection. (A) Densitometry analysis for phospho-eIF2alpha levels. Neuro2A cells non-transfected (NT) were used as control; cells treated with PERKi 200nM presents a significant decrease of phospho-eIF2alpha levels; and cells transfected with shPERK does not present any significant changes. **(B)** Densitometry analysis for eIF2alpha levels. Once again, neuro2A cells non-transfected were used as control and cells treated with PERKi 200nM or transfected with shPERK do not lead any significant alterations in eIF2alpha levels. **(A-B)** Each phospho-eIF2alpha or eIF2alpha line was normalized to the tubulin loading control band. Results were expressed as phospho-eIF2alpha or eIF2alpha/tubulin ratio. Values are expressed as mean ± SEM, n=4 independent experiments. **P<0.01 (Unpaired Student's t-test).

It was observed that neuro2A cells transfected with shPERK do not seem to cause any modification in phospho-eIF2alpha and eIF2alpha levels. Nevertheless, neuro2A cells treated with PERKi 200nM for 48h presented reduced levels of phospho-eIF2alpha but not of eIF2alpha levels. These results could mean that PERKi is acting in the inhibition of the PERK, which is in accordance with previous studies (Kim *et al.*, 2014).

It was noted that eIF2alpha levels in every study performed in this entire investigation do not exhibit any change (data not showed). Even in neuro2A transfected with different DNAs (e.g. Q22 or Q58); co-transfected with two different DNAs (e.g. Q22 co-transfected with shPERK); treated with PERKi and sodium arsenite (SA); and treated with PERKi or SA and transfected with some DNA (e.g. transfected with Q58 and treated with PERKi or transfected with Q22 and treated with SA).

3.3 Global translation levels are modulated by PERK inhibition and stress granules assembly

Some authors suggested that upon cellular stress, the translation process might be arrested and the protein synthesis decreases significantly (Anderson and Kedersha, 2002). To clarify if the induction of SGs with SA, PERKi and shPERK in fact contributes to translational arrest, we performed an assay to detect global protein synthesis levels. This puromycin-based assay described by Schmidt et al., 2009, is a useful and simple method to measure translation levels. Puromycin is an aminonucleoside antibiotic produced by *Streptomyces alboniger*, and a structural analog of aminoacyl tRNAs, which is incorporated into the nascent polypeptide chain and prevents elongation (Nathans, 1964). When used in minimal amounts, puromycin incorporation in neosynthesized proteins reflects directly the rate of mRNA translation *in vitro*. Then a monoclonal antibody against puromycin is used to directly monitor translation levels. For that, neuro2A cells were treated with SA 0,05mM for 1h; treated with PERKi 200nM for 48h; transfected with shPERK; and puromycin (10µg/ml) was added to all conditions, during the last 10 minutes of incubation, and cycloheximide (CHX) was used as positive control **(Fig. 9A-B)**.

We observed that upon stress granules assembly, through SA treatment, the levels of protein translation had a significantly decrease **(Fig. 9A-B)**. This is in agreement with the literature, reporting that SGs induction inhibits the translation process (Anderson and Kedersha, 2006; Kedersha and Anderson, 2007).

Upon PERKi treatment we did not detect any significant modification in the levels of protein translation **(Fig. 9A-B)**. One branch of the unfolded protein response results in the transient repression of protein synthesis via the phosphorylation of PERK, which in turn phosphorylates eIF2α. eIF2α-P prevents the formation of ternary complex, blocking translation at the level of initiation. Dephosphorylation of eIF2α-P allows protein synthesis to resume. Lowering eIF2α-P levels by PERKi completely restored vital protein synthesis rates (Scheper and Hoozemans, 2013; Halliday *et al.*, 2015).

Finally, we also saw that shPERK transfection, leads to a significant decrease in the levels of protein translation **(Fig. 9A-B)**.

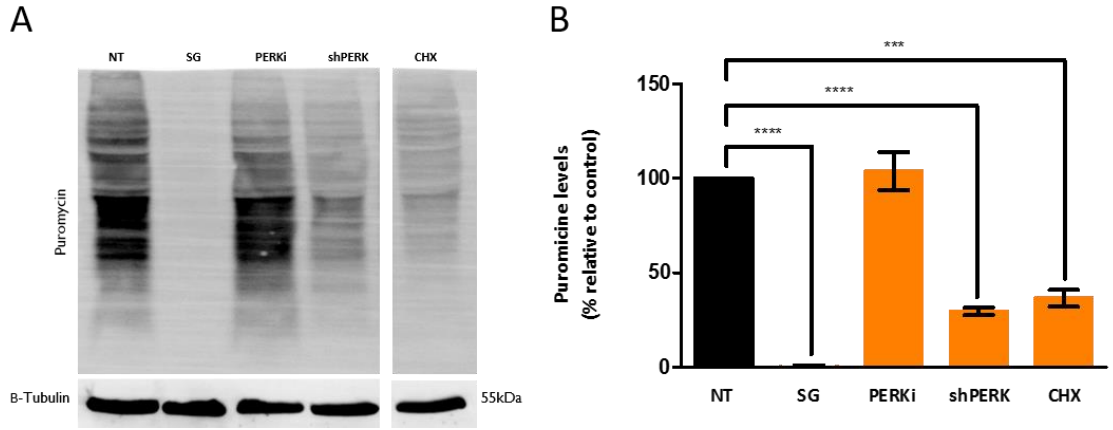

Figure 9 - Stress granules assembly and PERK inhibition modulates the global protein translation levels in neuro2A cells. (A) Western blot analysis probed for puromycin of neuro2A cells lysates of non-transfected cells (NT); treated with 0.05mM of sodium arsenite (SG); treated with 200nM of PERKi (PERKi); transfected with shPERK; and treated with cycloheximide (CHX). **(B)** Optical densitometry analysis for puromycin levels. A significant decrease of puromycin incorporation in the cells treated with SA is observed, and also in the shPERK transfected cells. Cells treated with PERKi does not show a significant modification of puromycin incorporation. Each puromycin line was normalized according to the tubulin loading control band. Results were expressed as puromycin/tubulin ratio. Values are expressed as mean ± SEM, n=4 independent experiments. ***P<0.001; ****P<0.0001 (Unpaired Student's t-test).

3.4 Stress granules assembly reduces the levels of ataxin 2 but not of ataxin 3

Upon SGs induction using SA, the translation is stopped, as previously demonstrated. We next aimed to evaluate how SGs assembly, induced by SA, correlates with the levels of WT ataxin-2, MUT ataxin-2, WT ataxin-3, MUT ataxin-3 and the levels of phospho-eIF2alpha.

We observed that SGs induction upon SA exposure affects the expression of ataxin-2 and ataxin-3, probably due to translation inhibition upon SGs assembly. When cells are exposed to SA, SGs are induced and some RBPs are recruited to these cytoplasmic granules, such as

TIA-1, G3BP1, PABP and ataxin-2. We observed a significant decrease in the levels of WT and MUT ataxin-2 **(Fig. 10A-B)**. Result of the association of ataxin-2 with PABP, that are translocated to the SGs, and it might be no longer available in the soluble form in the cytoplasm, and for that, the detected levels are significantly reduced (Kedersha and Anderson, 2007).

As for ataxin-3, there is no significant alteration of both WT and MUT forms of this protein upon SGs assembly, as observed in Fig. 10D-E. It also observed that phospho-eIF2alpha levels in cells transfected with WT and MUT ataxin-3 or ataxin-2 show an increase in cells treated with SA **(Fig. 10F)**.

This general reduction in ataxin-2 levels could be the result of the reduction in the translation rate, which results from SGs assembly. It also showed the levels of phospho-eIF2alpha were significant increase in transfected ataxin-2 cells treated with SA **(Fig. 10C)**. As previously mentioned, upon SGs assembly, the eIF2α was phosphorylated. So, levels of phospho-eIF2alpha increase, blocking the translation. No alterations were observed in ataxin-3 levels, because this protein were not recruited to SGs assembly, only the ataxin-2 and others mentioned proteins.

Taken together, these results show that the SA induction of SGs is able to modulate and alter the levels of ataxin-2 and phospho-eIF2alpha, which could suggest that this pathway might be important in the context of disease caused by these proteins.

Mouse endogenous levels of ataxin-2 and ataxin-3 were also analyzed and did not show any alteration in any experiment (data not showed).

Phospho-eIF2alpha levels were the similar in all experiments (data not showed). Neuro2A cells treated with PERKi show a decrease in phospho-eIF2alpha levels, as previously mentioned. In contrast, neuro2A cells treated with SA, the phospho-eIF2alpha levels were increase. This increase is more significant in cells previously transfected with WT and MUT ataxin-2 than with transfected WT and MUT ataxin-3.

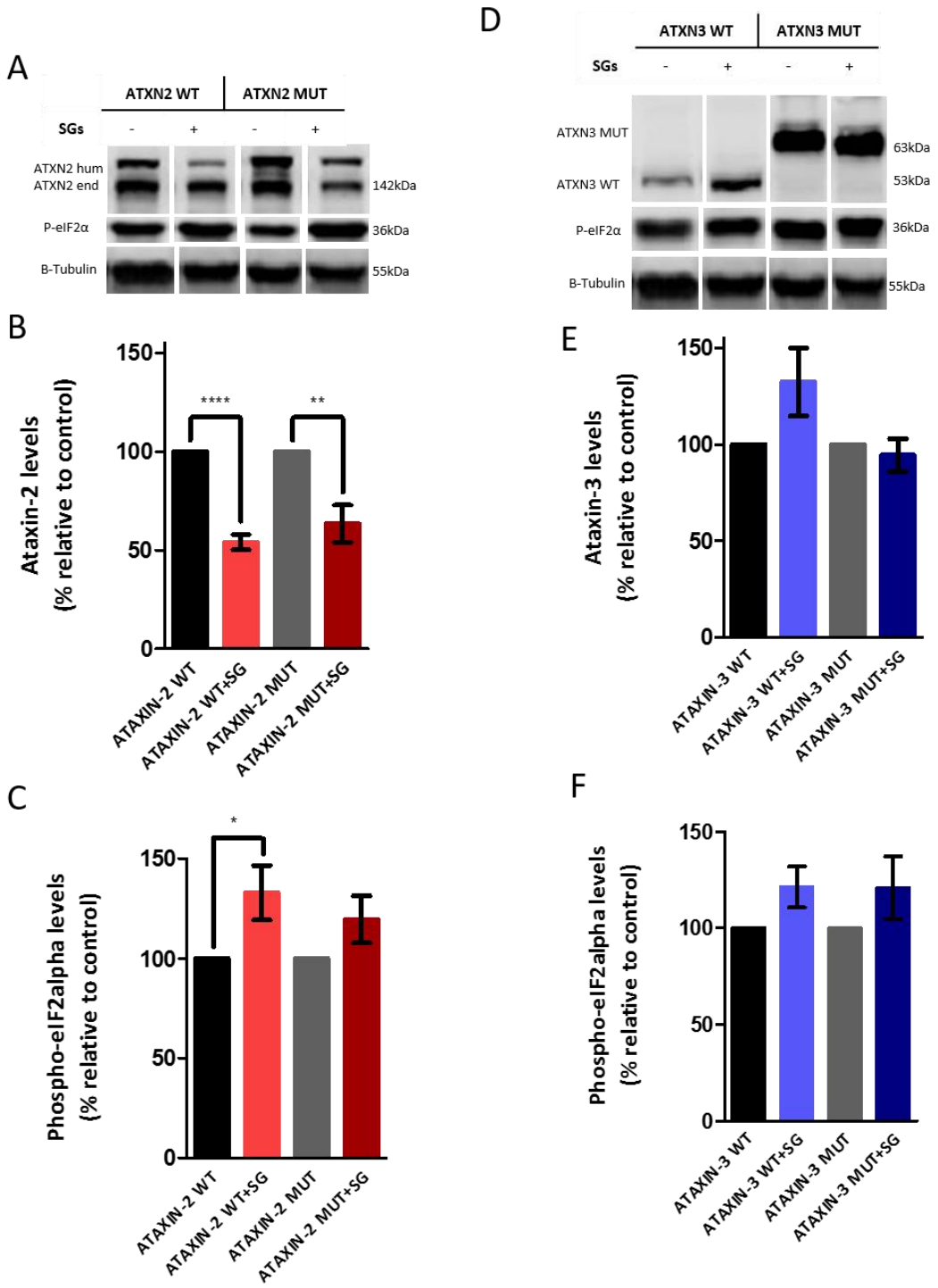

Figure 10 - Induction of SGs with sodium arsenite modulates the levels of ataxin-2 and ataxin-3 in neuro2A cells. Western blotting analysis of lysates of neuro2A cells previously transfected with ataxin-2 (WT and MUT) or ataxin-3 (WT and MUT), and treated with SA 0.05mM for 1h; and neuro2A cells only transfected with ataxin-2 (WT and MUT) or ataxin-3 (WT and MUT). **(A)** Western blot probed for ataxin-2 (MW: 142kDa), phospho-eIF2alpha (MW: 36kDa) and tubulin (MW: 55kDa). **(B)** Densitometry quantification for ataxin-2. Significant decrease of ataxin-2 levels in cells treated with SA. **(C)** Densitometry quantification for phospho-eIF2alpha. Significant increase of phospho-eIF2alpha levels in cells transfected with WT ataxin-2 (Q22). **(D)** Western blot probed for ataxin-3 (MW of WT ataxin-3: 53kDa and MW of MUT ataxin-3: 63kDa), phospho-eIF2alpha and tubulin. **(E)** Densitometry quantification for ataxin-3. No significant alterations in levels of ataxin-3 was observed. **(F)** Densitometry quantification for phospho-eIF2alpha in cells transfected with WT and MUT ataxin-3. It is observed an increase of phospho-eIF2alpha levels in cells treated with SA, but not significant considered. **(A-F)** Each ataxin-2 or ataxin-3 or phospho-eIF2alpha line was normalized to the tubulin loading control band. Results were expressed as ataxin-2 or ataxin-3 or phospho-eIF2alpha/tubulin ratio. Values are expressed as mean ± SEM, n=11 independent experiments. *P<0.05; **P<0.01; ****P<0.0001 (Unpaired Student's t-test).

In recent years, it has been broadly studied how mutant forms of ataxin-2 and ataxin-3 aggregate and cause neuropathology, which ultimately leads to cell death in SCA2 and SCA3/MJD, respectively (Durr, Pierre and De, 2010). Thus, we next wanted to address the effect of SGs induction by SA in ataxin-2 and ataxin-3 aggregation.

In neuro2A cells we observed, both WT and MUT forms of the proteins ataxin-2 and ataxin-3, have propensity to aggregate **(Fig. 11)** (Wolozin, 2014). As expected, this aggregation is much stronger upon transfection with the mutant forms.

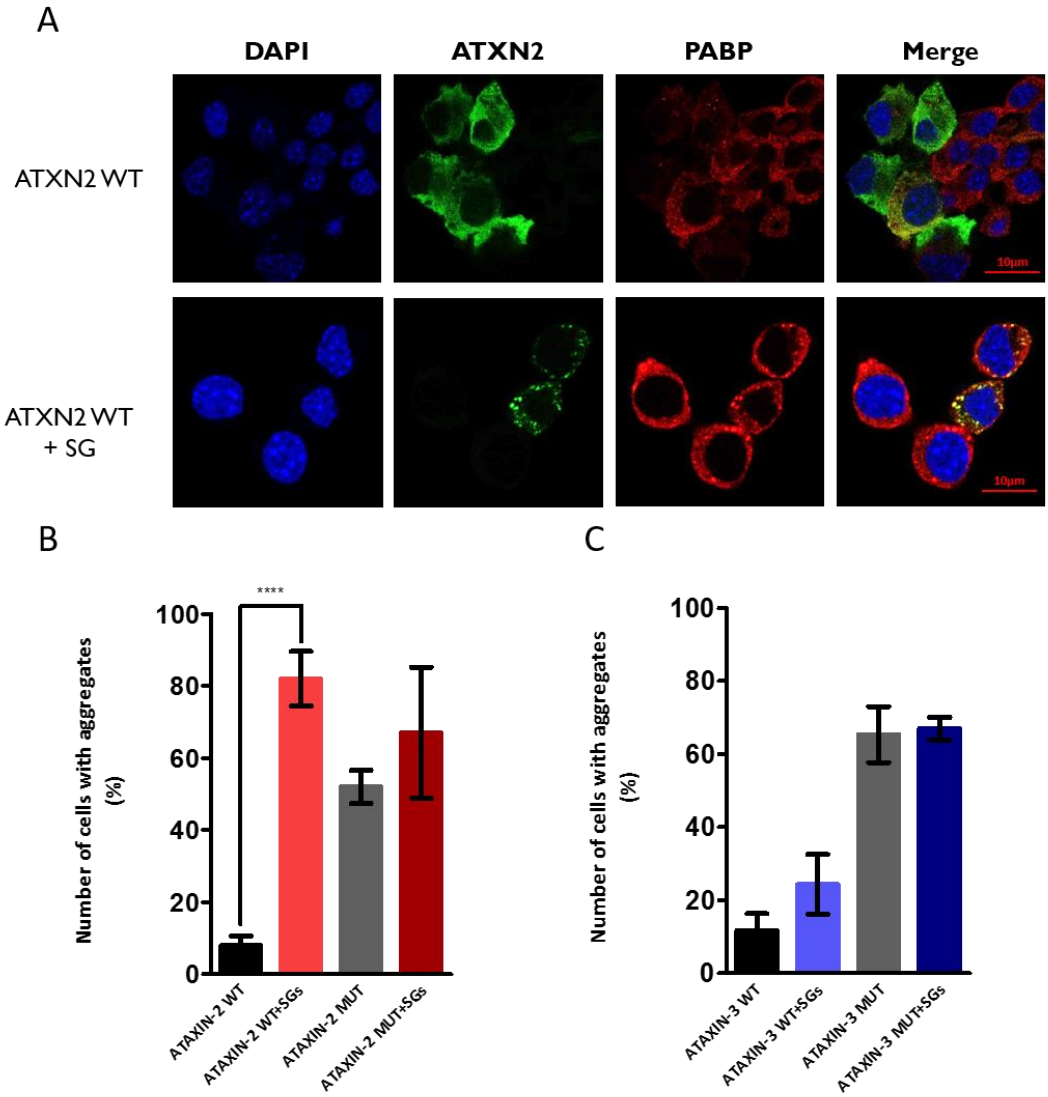

Figure 11 - SGs assembly affects ataxin-2 and ataxin-3 aggregation. Upon SA induce SGs assembly, the number of cells with aggregates increase significantly in WT and MUT ataxin-2, more relevant increase in WT ataxin-2 **(B)**. The number of cells (transfected with WT and MUT ataxin-3) with aggregates upon treated with SA increase but not with the same magnitude than with ataxin-2 **(C)**. Neuro2A cells were transfected with the following DNAs: GFP-WT ataxin-2, GFP-MUT ataxin-2, GFP-WT ataxin-3, GFP-MUT ataxin-3, and in certain conditions treated with SA 0.05mM to induce SGs. Cells were then stained with DAPI and the number of cells with aggregates were quantified directly in the microscope (63x), in a field within 100 random transfected cells. Representative images are shown **(A)**. Values are expressed as mean ± SEM, n=3 independent experiments. ****$p<0.0001$ (One-way ANOVA).

In ataxin-2, SA-induced SGs formation appears to play a role in aggregation, which occurs in both forms of the protein, WT and MUT. We observed an increase in the aggregation of ataxin-2 when cells are exposed to SA **(Fig. 11)**. The cells transfected with WT ataxin-2 showed a highly significant increase compared with MUT ataxin-2.

In ataxin-3, SA-induced SGs formation seems to not interfering in aggregation, in both forms WT and MUT.

As previously explained, as SGs are assembled, disease-causing proteins and RBPs (such as Ataxin-2, PABP, TDP-43 and FUS), are sequestered to SGs, where they interact significantly, which will lead to a more stable aggregation. Upon stress, (such as SA induced stress) and when pathologically expanded, these proteins form fibrils and irreversible pathological modifications occur (Wolozin, 2012). As we mentioned ataxin-3 is not a RBP to be sequestered to SGs, reason why SGs formation (SA induced) seems to have no impact in the ataxin-3 aggregation.

3.5 Ataxin 2 is recruited to stress granules upon stress induction but not ataxin 3

It is described in some studies that ataxin-2 is recruited to SGs and interacts with PABP (component of SGs), affecting and regulating the SGs formation (Anderson and Kedersha, 2007; Li *et al.*, 2013). Besides causing SCA2 when it is mutated, ataxin-2 has been show that interacts with ataxin-3, which in its mutated form cause MJD (Nóbrega *et al.*, 2015). With these data, is important to study the subcellular localization of these proteins upon SGs assembly.

We observed that neuro2A cells transfected with GFP-ataxin-2 co-localizes with SGs, induced by SA 48h after transfection (both forms: GFP-ataxin-2 WT and GFP-ataxin-2 MUT). Whereas the neuro2A cells transfected with GFP-ataxin-3 does not co-localizes with SGs (also in both forms: GFP-ataxin-3 WT and GFP-ataxin-3 MUT) **(Fig. 12)**. We can clearly see that in the ataxin-2 aggregates, there is also PABP (SGs marker), meaning that ataxin-2 is recruited to the SGs. With ataxin-3 that does not happen, and ataxin-3 aggregates does not overlap with the PABP.

What we observed is consistent with the literature, as the ataxin-2 is involved and recruited in SGs formation. About the interaction between ataxin-2 and ataxin-3, we know that ataxin-2 interacts with ataxin-3 and affect its function and pathology upon being recruited to

mutant ataxin-3 aggregates in MJD (Nóbrega *et al.*, 2015), it might not be recruited along with Ataxin-2 to the cytoplasmic granules. Although, the mechanism on how ataxin-2 is translocated to SGs is not yet fully elucidated.

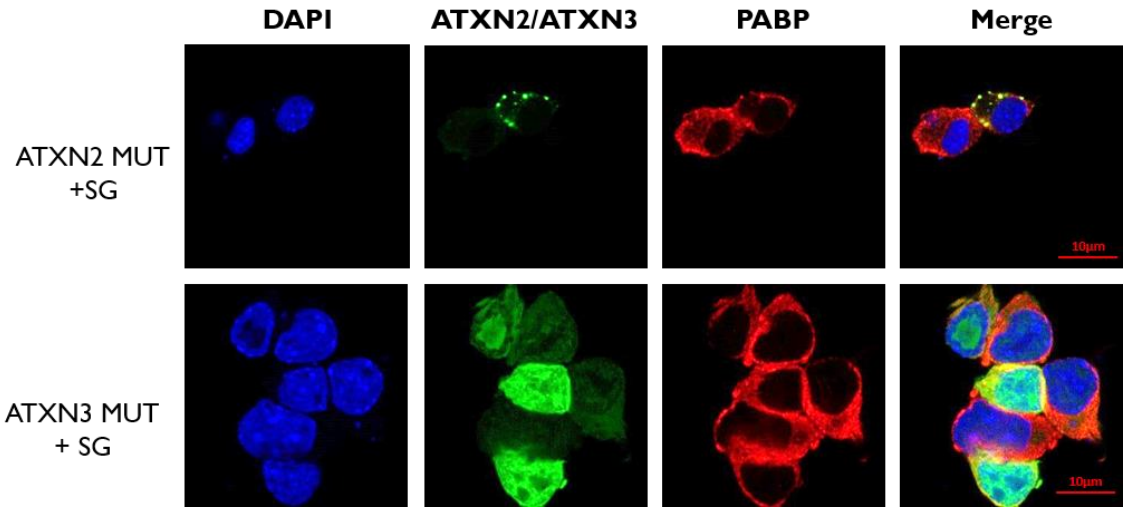

Figure 12 - Ataxin-2 is recruited to SGs but not ataxin-3. Neuro2A cells exposed to SA (to induce SGs formation), previously transfected with GFP-ataxin-2 (either WT and MUT) and GFP-ataxin-3 (either WT and MUT). An immunostaining assay was performed with anti-PABP antibody (SGs marker) and nuclei with DAPI. Representative confocal images from two different experiments show co-localization of SGs with GFP-ataxin-2, whereas GFP-ataxin-3 does not co-localize with SGs.

3.6 Inhibition of PERK leads to a significant reduction in the levels of both ataxin 2 and ataxin 3

As previously mentioned, ataxin-2 is component of SGs, upon SGs assembly. In this set of experiments, we aimed to address the effect of PERK inhibition in ataxin-2 and ataxin-3 levels in neuro2A cells, by PERKi treatment and shPERK transfection.

We observed that PERK inhibition, upon treatment with PERKi, leads to a significant reduction in both forms (WT and MUT) of ataxin-2 and ataxin-3 protein levels **(Fig. 13A-D)**. It is also showed that cells co-transfected with MUT ataxin-3 and shPERK, the shPERK causes a significant decrease in ataxin-3 levels, but not in WT ataxin-3. This result was not observed in WT and MUT ataxin-2 co-transfected with shPERK **(Fig. 13A-D)**.

The treatment with PERKi in this experiments result in a significant decrease of ataxin-2 and ataxin-3 levels, which was not expected by the previously results obtained. In theory, PERK inhibition should lead to an increase of soluble ataxin-2 and ataxin-3 levels. One of the last results demonstrated that PERK inhibition maintain the translation rate, and other result showed upon stress granules induction the ataxin-2 and ataxin-3 levels were decreased, probably translocated to aggregates. Moreover, it is known that upon stress granules

induction, PERK is activated to phosphorylates eIF2alpha, blocking translation. So when we inhibit the PERK by PERKi treatment: translation should work normally; SGs assembly should be inhibited, proteins were not recruited to SGs. Facts that contribute to increase soluble ataxin-2 (mainly, because is known that it is recruited to SGs) and ataxin-3 levels. On the other hand, exist one study proving that PERK activation and inactivation induce the autophagy in cells. They don't conclude the specific interaction between PERK and autophagy, but they observe alterations (Avivar-valderas *et al.*, 2011). In our case, we can also suspect in this interaction between autophagy and PERK. Somehow, PERK inhibition could activate autophagy and cause the reduction of ataxin-2 and ataxin-3 levels.

Next aim was to study the effect of PERK inhibition in ataxin-2 and ataxin-3 aggregation, upon PERKi treatment. As mentioned before, WT and MUT forms of the proteins ataxin-2 and ataxin-3 have propensity to aggregate, namely in the mutated forms.

PERKi treatment significant decreased MUT ataxin-2 aggregation, and also significant decreased MUT ataxin-3 aggregation **(Fig. 13E-G)**. This effect is very clear in the mutated forms of both ataxin-2 and ataxin-3, compared to the WT forms of both proteins.

As previously explained, when these proteins form fibrils and irreversible pathological modifications (aggregates) the SGs assembly were also associated in aggregation, and lead to formation of more stable complexes. It is also previously mentioned that PERKi treatment decreases SGs assembly by PERK inhibition. Further ahead it is demonstrated that the levels of P62 were reduced upon PERKi treatment, leading to activation of autophagy. And when autophagy was activated the aggregates were decreased. Then, somehow these results were expected. Where PERK inhibition were performed, the number of cells with aggregates must decrease (as been showed). Because SGs assembly were blocked by PERK inhibition, leading a decrease of aggregation.

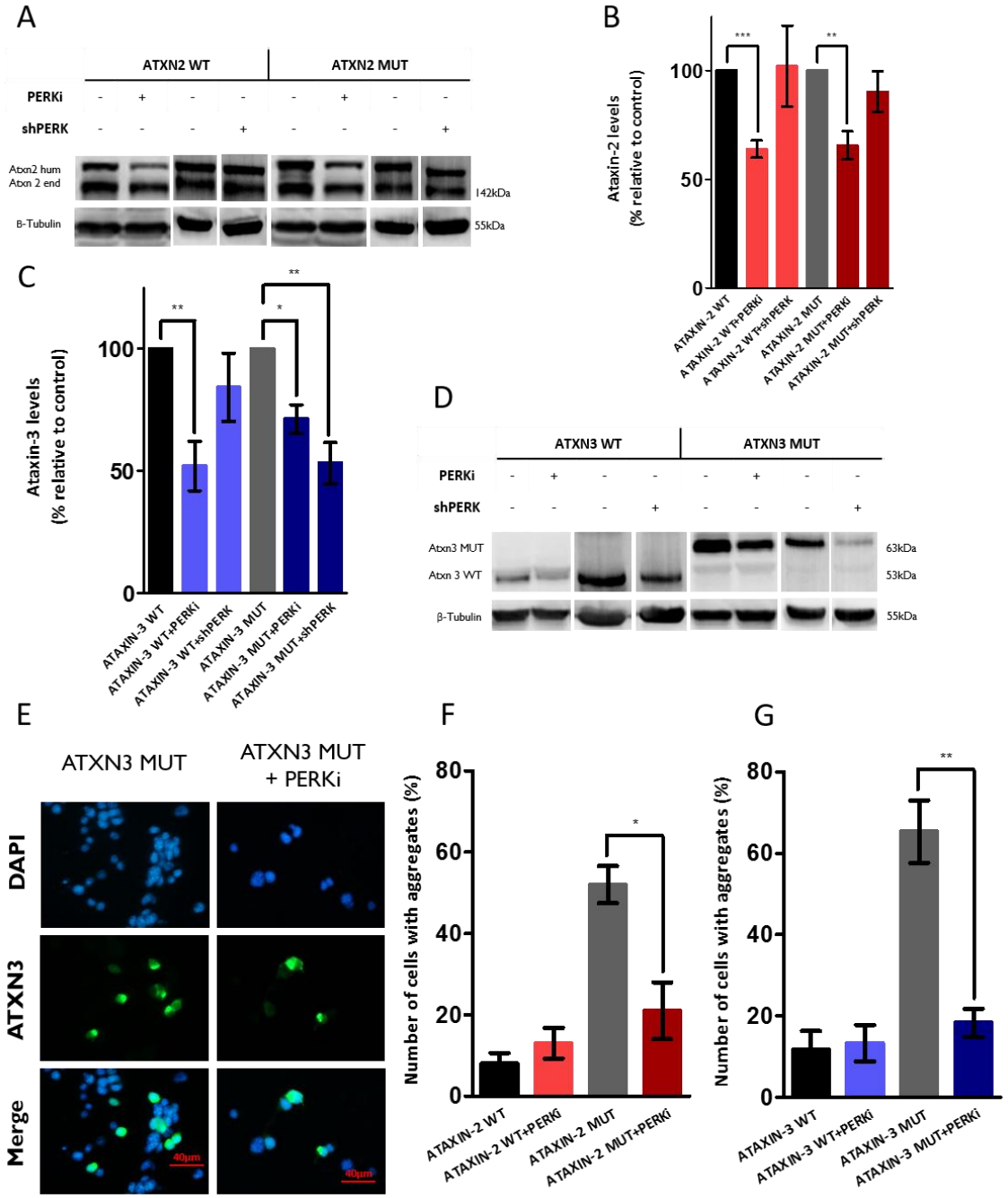

Figure 13 - Inhibition of PERK significantly reduces the levels of ataxin-2 and ataxin-3 in neuro2A cells, as aggregation of its mutated forms. (A-D) Western blot analysis probed for ataxin-2 **(A)**, ataxin-3 **(C)** and tubulin **(A, C)**. Densitometry quantification for ataxin-2 **(C)** and ataxin-3 **(D)**. Neuro2A cells were previously transfected with WT and MUT ataxin-2 or WT and MUT ataxin-3. In specific conditions a co-transfection occur with both forms of ataxin-2 or ataxin-3 and shPERK; and in different conditions cells, previously transfected with WT and MUT ataxin-2 or ataxin-3, were treated with PERKi 200nM. It is showed a significant decrease of ataxin-2 and ataxin-3 levels upon treatment with PERKi. In contrast, only in cells co-transfected with MUT ataxin-3 and shPERK, the shPERK causes a significant decrease in ataxin-3 levels. The remaining conditions don´t have significant alterations. Each ataxin-2 or ataxin-3 line was normalized to the tubulin loading control band. Results were expressed as ataxin-2 or ataxin-3/tubulin ratio. Values are expressed as mean ± SEM, n=5. *P<0.05; **P<0.01; ***P<0.001 (Unpaired Student's t-test). **(E-G)** Number of cells with aggregates in both forms of ataxin-2 and ataxin-3. PERKi treatment significant decreased MUT ataxin-2 aggregation **(F)**, and also significant decreased MUT ataxin-3 aggregation **(G)**. Representative images are show **(E)**. Cells were then stained with DAPI and the number of cells with aggregates were quantified directly in the microscope (63x), in a field within 100 random transfected cells. Values are expressed as mean ± SEM, n=3 independent experiments. *p<0.05; **P<0.01 (One-way ANOVA).

3.7 Combined effect of the inhibition of PERK and stress granules assembly reduces the levels of ataxin 2 and ataxin 3

Next, we aimed to investigate the combined effect of the induction of SGs using SA and the inhibition of PERK, by PERKi treatment. These set of experiments showed a significant decrease of ataxin-2 and ataxin-3 levels upon combined treatment with PERKi and SA **(Fig. 14C-D)**. In contrast, only in cells co-transfected with MUT ataxin-3 and shPERK, the shPERK causes a significant decrease in ataxin-3 levels **(Fig. 14D)**. The remaining conditions do not have significant alterations.

As previously demonstrated the levels of ataxin-2 and ataxin-3 were significant decreased upon PERK inhibition by PERKi treatment. And only in cells co-transfected with MUT ataxin-3 and shPERK these levels were also significant decreased. These results demonstrate that the results were consistent with the anterior results and upon PERK inhibition with or without SGs induction (SA treatment) the levels of ataxin-2 and ataxin-3 decrease in the same conditions.

In the next experiment we wanted to investigate how the combined effect of SGs assembly and PERK inhibition affects ataxin-2 and ataxin-3 aggregation.

PERKi treatment combined with SA treatment significant decreased WT and MUT ataxin-2 aggregation, compared with cells only treated with SA **(Fig. 15B)**. It also showed a significant decreased MUT ataxin-3 aggregation upon combined treatment of PERKi and SA **(Fig. 15C)**.

As previously explained, SA treatment causes SGs assembly, and upon this stress ataxin-2 and ataxin-3 aggregates in a stable form. Although PERKi treatment leads to a PERK inhibition, and this inhibition reduces the number of cells with aggregates. So, as predicted, the combined effect of SGs assembly and PERK inhibition show a strongly decreased aggregation of ataxin-2 and ataxin-3.

Altogether, these aggregation results studied suggest that SGs induction by SA treatment exerts the main role in aggregation in these cellular disease models. In the same line, it was shown that oxidative stress plays an important role in the pathogenesis of neurodegenerative disorders, including ataxias. Furthermore, oxidative stress acts as co-factor, namely in SCA2. In aggregation, activation of apoptosis/caspases, autophagy, calcium and dopaminergic signalling, endoplasmic reticulum signalling, gene transcription, heat shock pathway, mitochondrial dysfunction, and synaptic neurotransmission deficits are involved

(Casetta, Govoni and Granieri, 2005; Guevara-garcía *et al.*, 2012). Some of these molecular mechanisms generate reactive species that in turn are messengers or mediators of the related process, which will ultimately lead to oxidative stress. Thus, we can postulate that an oxidative stress environment is prone to aggregation in a SCA2 cellular model but not in a SCA3 cellular model. And PERK inhibition seems to have a key role in decrease aggregation in both SCA2 cellular model and SCA3 cellular model. Even when exists combined effect of PERK inhibition and SGs assembly (in SCA3 cellular model only appears this results in MUT ataxin-3 conditions).

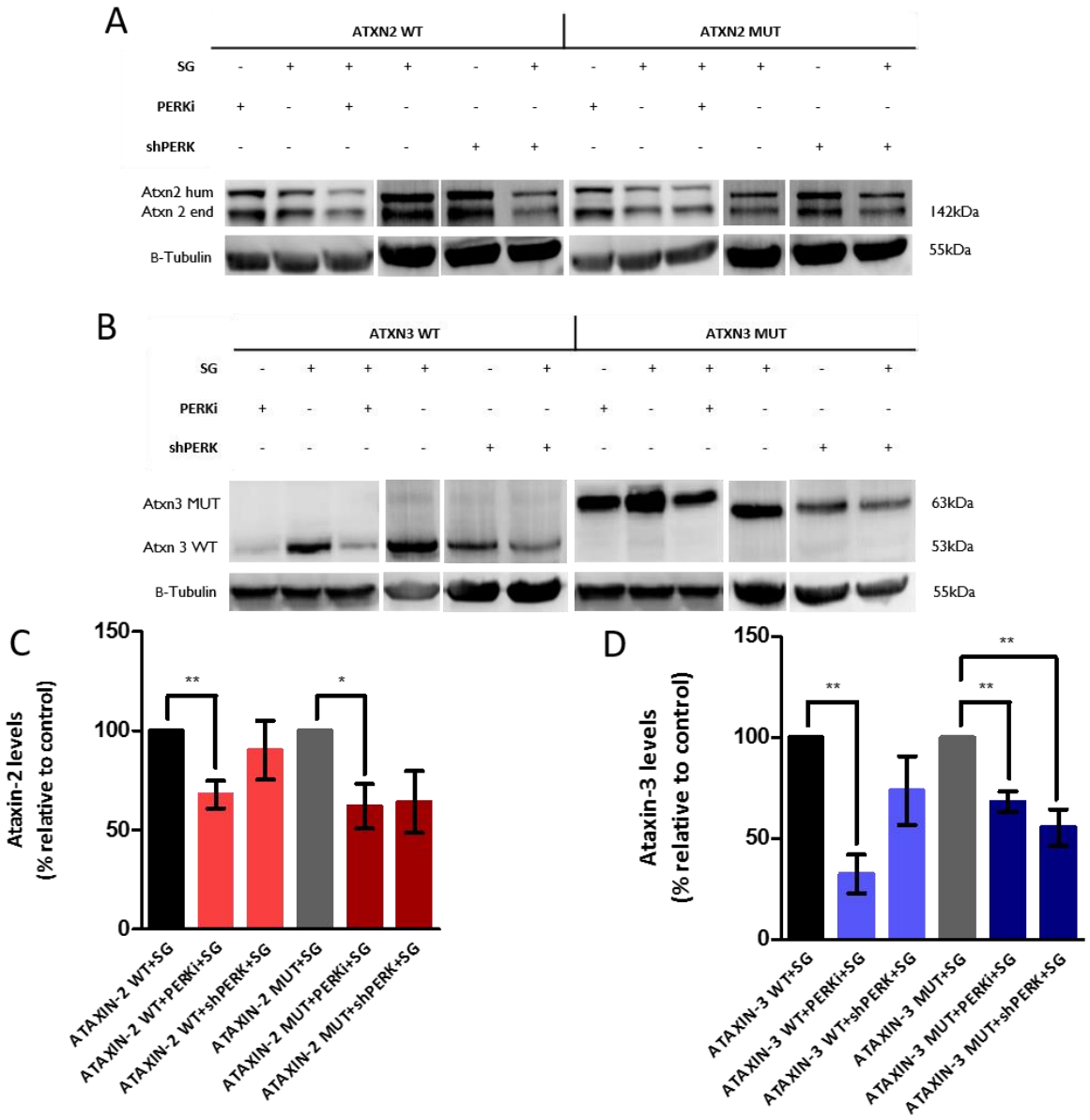

Figure 14 - Combined effect of PERK inhibition and SGs assembly reduces the levels of ataxin-2 and ataxin-3 in neuro2A cells. Western blot analysis probed for ataxin-2 **(A)**, ataxin-3 **(B)** and tubulin **(A, B)**. Densitometry quantification for ataxin-2 **(C)** and ataxin-3 **(D)**. Different conditions were analyzed: cells previously transfected with WT and MUT ataxin-2 or ataxin-3 and treated with SA 0.05mM; cells previously transfected with WT and MUT ataxin-2 or ataxin-3 and treated with PERKi combined with SA; and cells previously co-transfected with WT and MUT ataxin-2 or ataxin-3 and shPERK, and treated with SA. It is

showed a significant decrease of ataxin-2 and ataxin-3 levels upon combined treatment with PERKi and SA **(C, D)**. In contrast, only in cells co-transfected with MUT ataxin-3 and shPERK, the shPERK causes a significant decrease in ataxin-3 levels **(D)**. The remaining conditions don´t have significant alterations. Each ataxin-2 or ataxin-3 line was normalized to the tubulin loading control band. Results were expressed as ataxin-2 or ataxin-3/tubulin ratio. Values are expressed as mean ± SEM, n=5 independent experiments. *P<0.05; **P<0.01; ***P<0.001 (Unpaired Student's t-test).

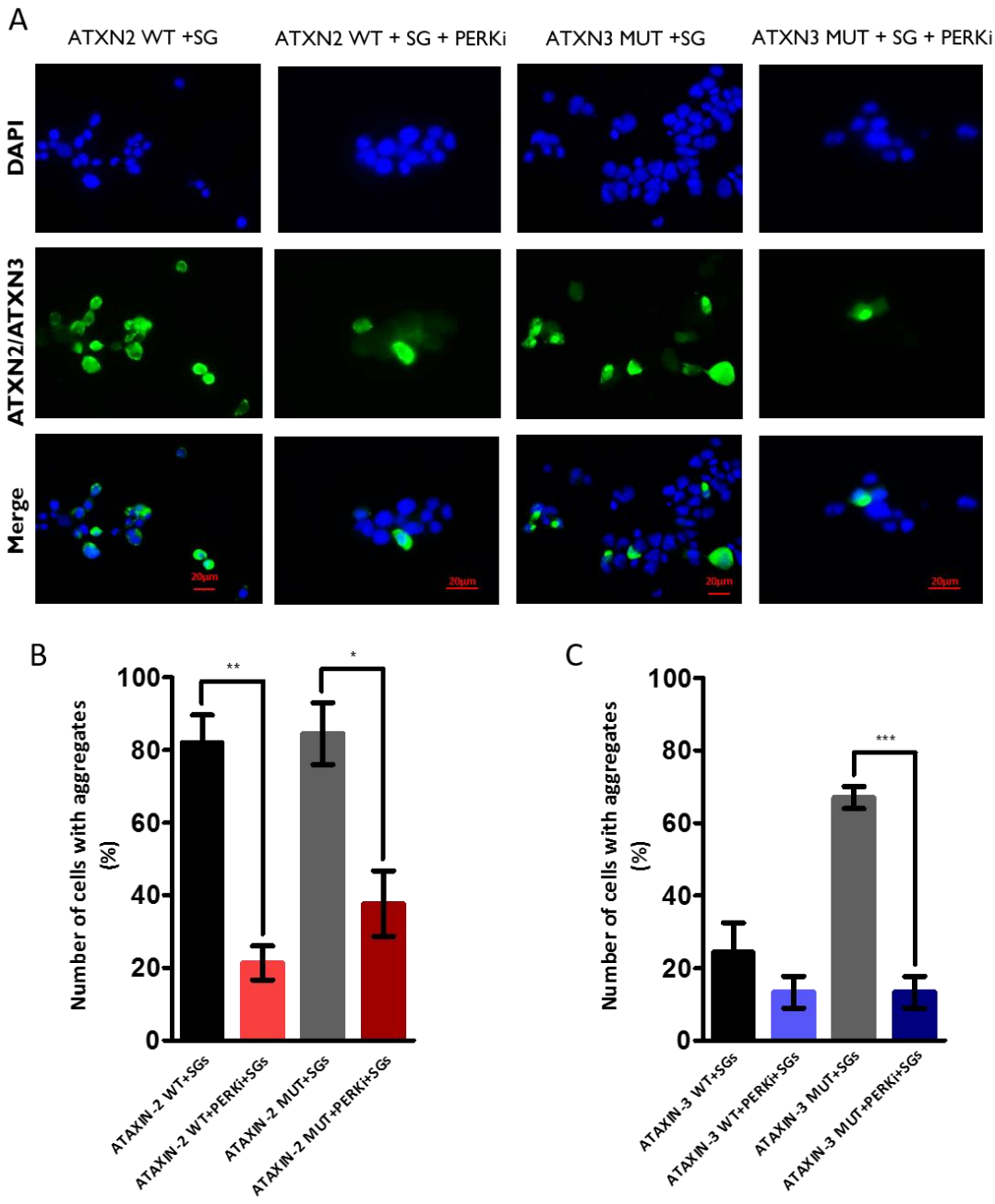

Figure 15 - Combined effect of PERK inhibition and stress granules assembly decrease aggregation of ataxin-2 and ataxin-3 in neuro2A cells. Number of cells with aggregates in both forms of ataxin-2 and ataxin-3. PERKi treatment combined with SA treatment significant decreased WT and MUT ataxin-2 aggregation, compared with cells only treated with SA **(B)**. It also showed a significant decreased MUT ataxin-3 aggregation upon combined treatment of PERKi and SA **(C)**. Representative images are show **(A)**. Cells were then stained with DAPI and the number of cells with aggregates were quantified directly in the microscope (63x), in a field within 100 random transfected cells. Values are expressed as mean ± SEM, n=3 independent experiments. *p<0.05; **P<0.01; ***P<0.001 (One-way ANOVA).

3.8 Reversion of stress granules induction upon PERK inhibition significantly decreases the levels of ataxin 2 but not ataxin 3

Previous studies have reported that when a stress is removed from cells, SGs are capable of disassemble (Anderson and Kedersha, 2002; Buchan and Parker, 2013). With this information, we wanted to investigate if, by removing the stress stimuli, we could re-establish ataxin-2 and ataxin-3 protein levels. Neuro2A cells were transfected with ataxin-2 (WT and MUT) and ataxin-3 (WT and MUT) and treated with PERKi. After 48 hours, we induced SGs with SA for 1 hour. After that, we removed the medium from our condition of interest, applied new medium and cells incubated for one more hour, and these conditions we namely "SGs removal" (±SGs).

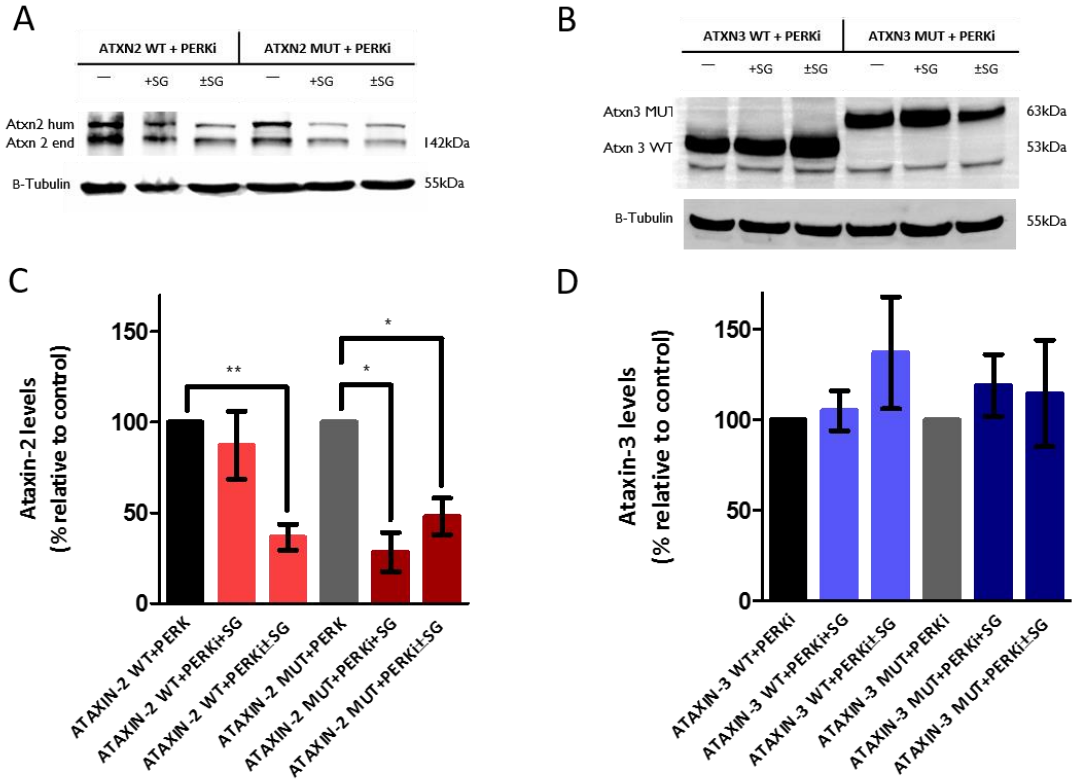

Figure 16 - Stress removal upon PERK inhibition does not re-establish ataxin-2 and ataxin-3 levels in neuro2A cells. (A) Western blot probed for ataxin-2. **(B)** Western blot probed for ataxin-3. **(C)** Densitometry quantification for ataxin-2. There is a slight reduction in ataxin-2 levels when SA is applied, which is significant in the case of MUT ataxin-2. When SA is removed from cells, proteins are not re-established to previous basal levels, but were also a significant decrease in ataxin-2 levels (in both forms). **(D)** Densitometry quantification for ataxin-3. No alteration in ataxin-3 levels were observed. **(A-D)** Neuro2A cells were transfected with WT ataxin-2 (Q22), MUT ataxin-2 (Q58), WT ataxin-3 (Q24) or MUT ataxin-3 (Q84), and after that cells were treated with PERKi. Each ataxin-2 or ataxin-3 line was normalized to the tubulin loading control band. Results were expressed as ataxin-2 or ataxin-3/tubulin ratio. Values are expressed as mean ± SEM, n=3 independent experiments. *P<0.05; **P<0.01 (Unpaired Student's t-test).

The stress removal does not re-establish the levels of ataxin-2 and ataxin-3, either WT or the MUT forms. As already mentioned, we observed an overall reduction in the protein

levels when the SA is applied, although it is not significant in the case of WT and MUT ataxin-3 **(Fig. 16)**. However, when re-establishing the normal conditions, the protein levels did not recover to its previous state. This might have occurred because the time cells had to recover from the stress was not enough for the protein translation to be re-established.

3.9 Autophagy marker is altered upon PERK inhibition or stress granules induction

Several evidences reveal that one of the areas where autophagy appears to be crucial is to prevent neurodegeneration and therefore, alterations in the different steps of this clearance process might be intimately linked to many human diseases. Intracellular protein aggregates and dysfunctional organelles are common features of neurodegenerative diseases, such as spinocerebellar ataxias (SCAs). In these disorders, the pathology is associated with the protein propensity to aggregate and accumulate. Therefore, in the presence of toxic proteins, autophagy upregulation has also been shown to be beneficial (Baumer *et al.*, 2014; Nascimento-Ferreira *et al.*, 2011; Nixon *et al.*, 2005; Seidel *et al.*, 2016).

Aiming to see if autophagy is altered upon PERK inhibition or SGs induction, we measured the levels of protein P62: in neuro2A cells non-transfected, transfected with WT and MUT ataxin-2 and transfected with WT and MUT ataxin-3.

P62 protein recognizes toxic cellular waste, which is then scavenged by autophagy. Lack of autophagy leads to accumulation of p62, which is not good for cells, as it induces a cellular stress response that could lead to disease. At first glance, p62 seems beneficial for the cell, ensuring aggregation and subsequent turnover of potentially harmful proteins by autophagy. But as usual, too much of a good thing can be bad (Rusten and Stenmark, 2010). Decreased levels of P62 seems to be good for the cells, and it is an indicator that autophagy is active and playing your role in cells.

We observe a significant decrease in P62 levels upon PERK inhibition, by treatment with PERKi 200nM. Only in neuro2A cells transfected with WT and MUT ataxin-3, the P62 levels not suffer any modification in all tested conditions. Even when cells are treated with PERKi or/and treated with SA 0.05mM **(Fig. 17)**.

Non-transfected cells were tested and acts as a control of this experiment. We observed that cells treated with PERKi presents a significant decrease of P62 levels, and cells treated with SA-induced SGs formation do not show any alteration in P62 levels. Even the cells

treated with both compounds (PERKi and SA) feature a significant decrease in P62 levels. These results are also observed in cells transfected with WT and MUT ataxin-2 and treated with PERKi and/or SA **(Fig. 17)**.

Taken together these results and the P62 information it was being showed that PERKi helps the cells homeostasis, by increasing the toxic compounds removed in autophagy.

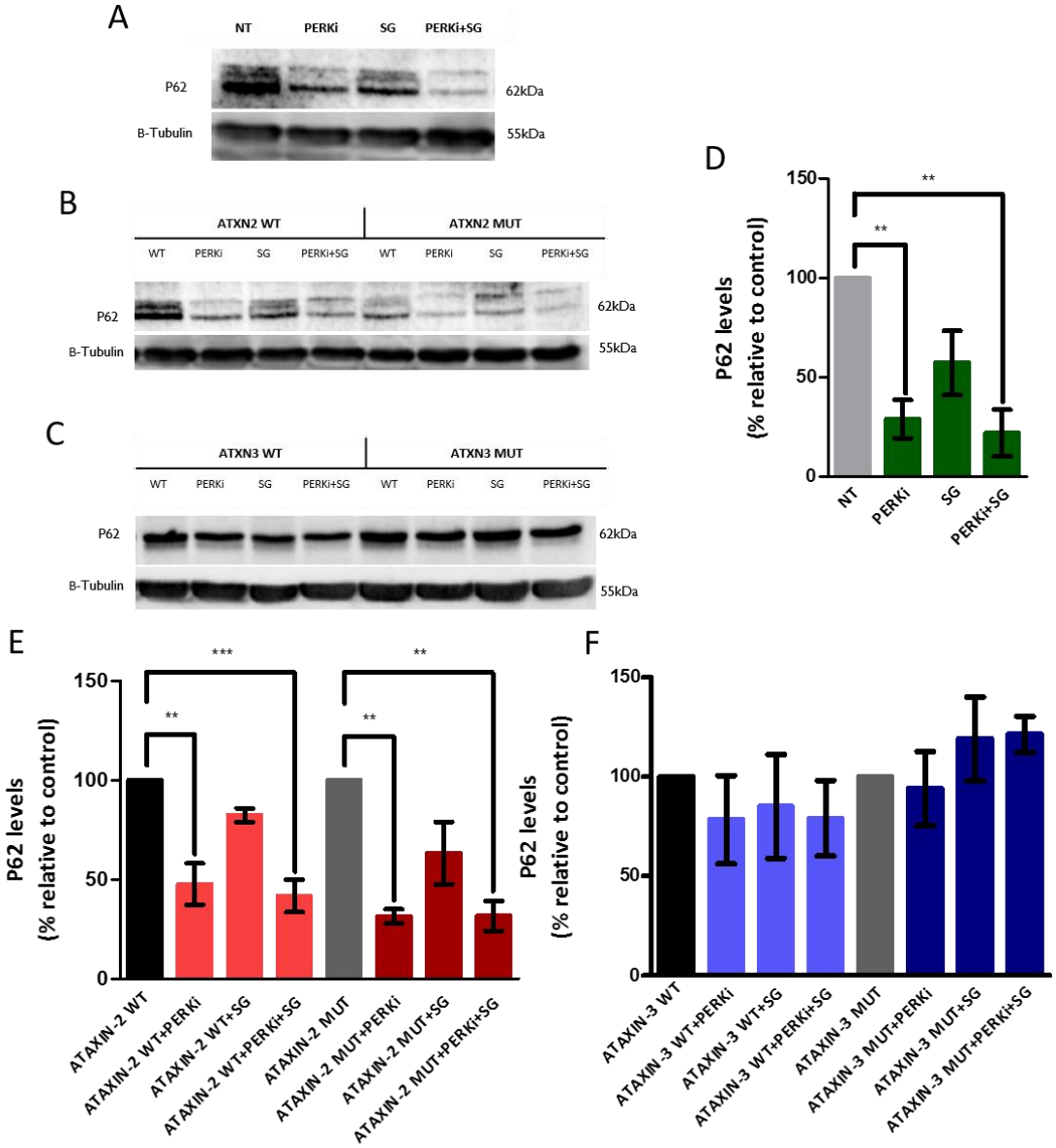

Figure 17 - P62 levels are reduced upon PERK inhibition in neuro2A cells. Western blotting analysis probed for P62. (MW: 62kDa) and tubulin (MW: 55kDa). **(A)** Western bolt analysis of non-transfected neuro2A cells. **(B)** Western blot analysis of neuro2A cells transfected with WT and MUT ataxin-2. **(C)** Western blot analysis of neuro2A cells transfected with WT and MUT ataxin-3. **(D-F)** Densitometry quantification for P62 of non-transfected cells **(D)**, cells transfected with ataxin-2 **(E)**, and cells transfected with ataxin-3 **(F)**. It is observed a significant decrease of P62 levels upon PERK inhibition, except in cells transfected with both forms of ataxin-3. This effect is also observed in cells with PERK inhibited and treated with SA-induced SGs formation. Each P62 line was normalized to the tubulin loading control band. Results were expressed as P62/tubulin ratio. Values are expressed as mean ± SEM, n=3 independent experiments. **P<0.01; ***P<0.001 (Unpaired Student's t-test).

3.10 *In vivo* expression of shPERK does not lead to any toxicity in the mouse striatum

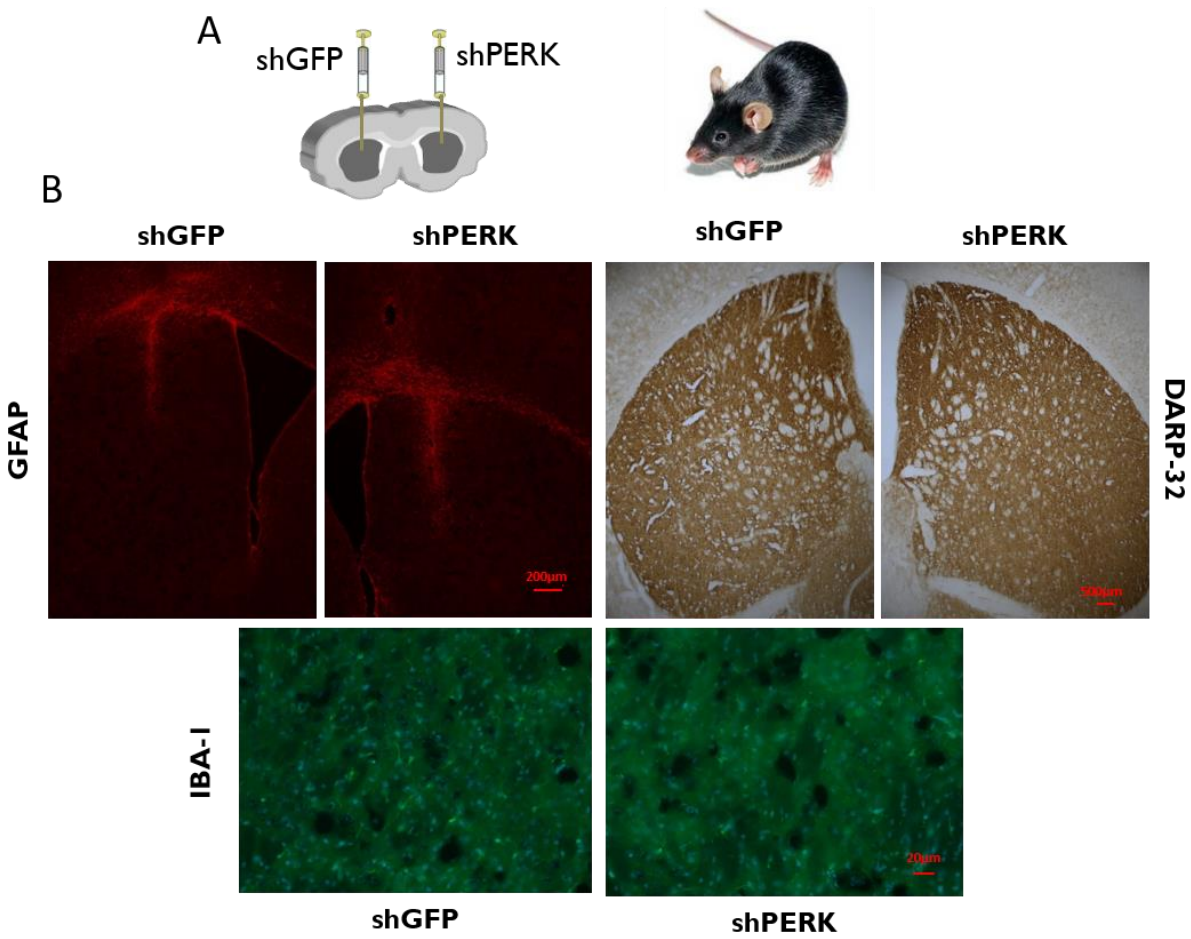

Figure 18 - shPERK has no effect in the astroglyosis, or microgliosis or neuronal loss. **(A)** Schematic representation of stereotaxic bilateral injection of lentiviral vectors in mice striatum. **(B)** Immunohistochemical staining of mice striatal sections for: microglia and astrocytes markers, Glial fibrillary acidic protein (GFAP) a marker for glial activation; for ionized calcium-binding adapter molecule 1 (IBA-1), a neuronal inflammation marker; and for neuronal nuclei protein DARP-32, a marker of neuronal loss. It is not observed any alteration upon shPERK injection. n=4.

Inflammation plays a two faced role in neurodegeneration. Can act as a first league mechanism defense or as causative of cell death (Amor *et al.*, 2010). In this study to further evaluate if shPERK could affect inflammation we performed an immunohistochemical analysis for some markers: iba-1 for microglia and GFAP for astrocytes. No differences were identified; which could indicate that shPERK does not act in neuroinflammation in this particular model **(Fig. 18)**.

To further investigate the effect of shPERK in the neuropathological features we performed immunohistochemistry staining a neuronal loss marker, the DARP-32. The lentiviral injection of shPERK did not produce any alteration in neuronal loss compared with the hemisphere injected with shGFP **(Fig. 18)**.

3.11 Expression of shPERK enhances the toxicity induced by mutant ataxin 3 in the mouse striatum

Finally, with the previous results, we aimed to address the effect of the shPERK expression in a MJD lentiviral mouse model.

As previously reported, mutant ataxin-3 is able to form ubiquinated aggregates when expressed in the mouse striatum. In order to investigate the effects of SGs in neuropathological features *in vivo*, we used a MJD lentiviral based mouse model, and overexpressed MUT ataxin-3 in one hemisphere and MUT ataxin-3 with shPERK in the other hemisphere **(Fig. 19A)** (Alves *et al.*, 2008). We stained the histological sections with DARP-32, a marker for neuronal degeneration, to investigate if shPERK expression was capable of reducing neuronal loss at 4 weeks post-injection. In fact, shPERK expression led to a significant increase of neuronal loss, thus not revealing a neuroprotective effect **(Fig. 19B-C)**.

Then, we proceed an immunohistological staining with ubiquitin to evaluate the MUT ataxin-3 aggregates. We observed an almost total reduction in the number of ubiquitin aggregates, comparing to the control hemisphere (data not showed). But when we perform these experiments it is noted one big degradation of histological sections. A new analysis was performed to evaluate the cells degradation. We made the cresyl violet staining in the mice striatal sections previously studied, and as expected it is revealed significant cell degradation when shPERK is expressed **(Fig. 19D)**. The results of the immunohistological staining with ubiquitin were rejected. There are no ubiquitin aggregates because exists a significant degradation of the striatum tissue.

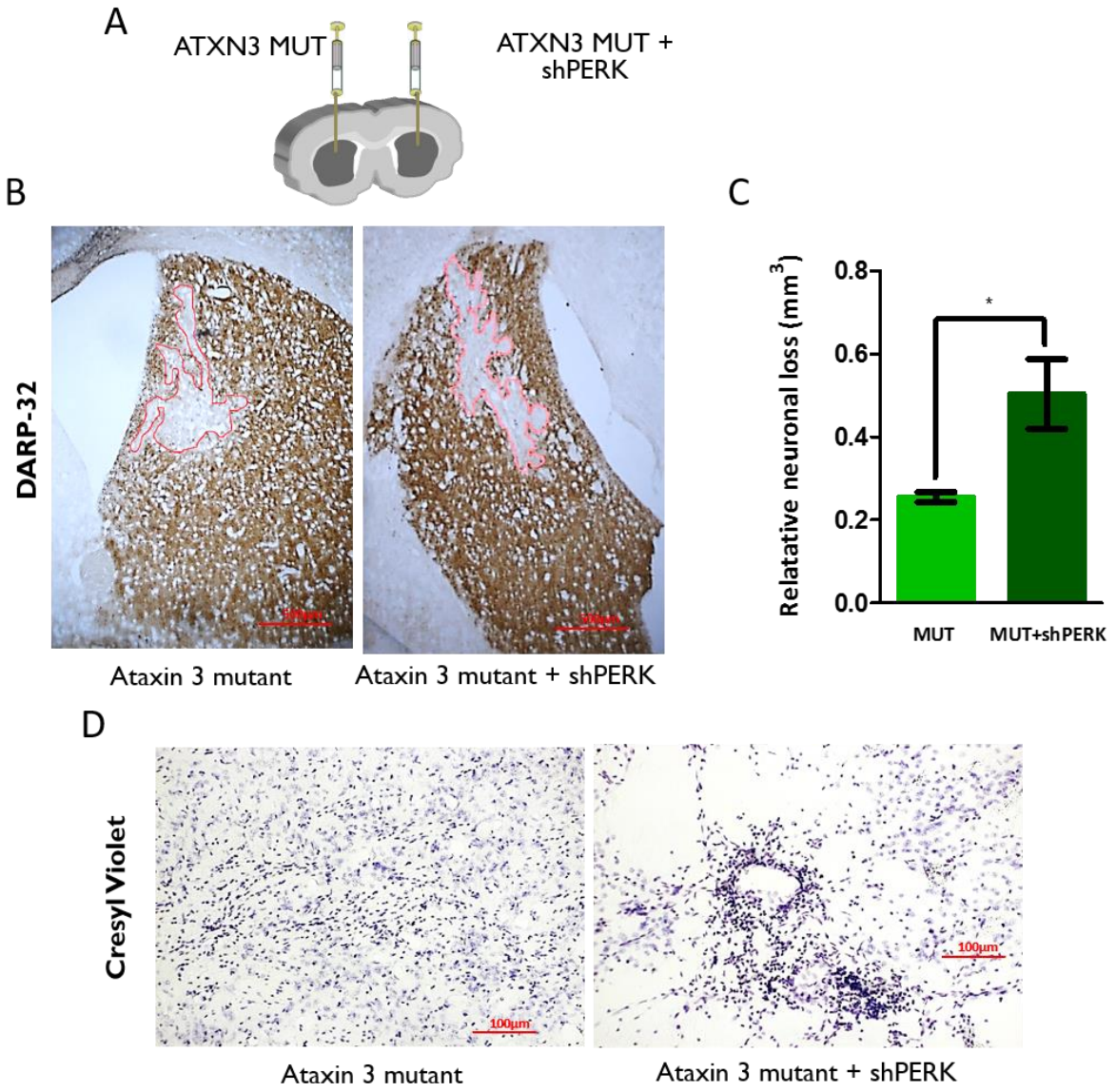

Figure 19 - shPERK expression in mouse striatum enhance toxicity induced by mutant ataxin-3. (A) Schematic representation of stereotaxic bilateral injection of lentiviral vectors in mice striatum. Lentiviral vectors encoding human MUT ataxin-3 with 72 glutamines (ATXN3 MUT) were injected in the striatum of 4 weeks old C57/Bl6 mice. **(B)** Immunohistochemical staining of mice striatal sections for DARP-32, marker of neuronal loss. **(C)** Quantification of DARP-32 depleted volume (mm3) 4 weeks after co-injection. It is observed neuronal loss upon shPERK expression. Values are expressed as mean ±SEM, n=8. *P<0.05 (paired Student's t-test). **(D)** Cresyl violet staining of mice striatal sections injected with MUT ataxin-3 and sections co-injected with MUT ataxin-3 and shPERK. It is revealed a significant cell layer degradation.

Taking into account these results, it seems that expression of shPERK enhances the toxicity induced by MUT ataxin 3 in the mouse striatum. The previous study reveals that lentiviral injection of shPERK alone does not reveal any toxicity in striatum (neuroinflamation and neuronal loss). But when we co-injected MUT ataxin-3 and shPERK we observe a significant increase of neuronal loss and a significant cell layer degradation. Somehow MUT ataxin-3 and shPERK interacts causing this toxicity. We could not achieve any resolution and explication for this occurrence, but some interaction between MUT ataxin-3 and shPERK is suspected by us.

CHAPTER IV – CONCLUSIONS AND PERSPECTIVES

4. Conclusions and future perspectives

In this study we addressed the effect of the PERK inhibition in a cellular model of SCA2 and SCA3 and in a lentiviral mouse model of SCA3. PERK is one of the kinases that phosphorylate the eIF2alpha, leading to SGs assembly. Considering that the SCA2-causing protein ataxin-2 is recruited to SGs and that it has been reported that this protein interacts with ataxin-3, affecting SCA3's pathology, it became important to study the effect of PERK inhibition in the context of these diseases, as well as investigating if SGs could have a significant role in a neurodegeneration context.

We observed that by inducing cellular stress (with SA), decrease significantly the levels of ataxin-2, having no significant effects in ataxin-3 levels. We can conclude that SGs induction reduce the levels of ataxin-2, given the fact that this protein is sequestered to SGs. We also observed that SGs assembly increases the number of ataxin-2 and ataxin-3 aggregates. As expected, the levels of phospho-eIF2alpha increase, as translation rate decrease. Thus, it is clear that an oxidative stress environment is prone to aggregation in a SCA2 cellular model.

We also observed that PERK inhibition by PERKi treatment, decreases significantly the levels of phospho-eIF2alpha but not the eIF2alpha levels, as expected. The translation rate was maintained upon PERK inhibition. PERK inhibition in a cellular model of SCA2 and SCA3, reduces significantly aggregation in both cellular models. Upon these results one unexpected result appears: a decrease in the levels of ataxin-2 and ataxin-3 upon PERKi treatment. The aggregation was decreased and the translation rate not altered, and somehow one could expect that soluble ataxin-2 and ataxin-3 increased. Another result obtained were the decrease in one autophagy marker (P62), upon PERK inhibition. These result could be one evidence that PERK inhibition leads to an induction of autophagy, and this activation decreases the levels of ataxin-2 and ataxin-3 and aggregation. That is our suspected theory.

The PERK inhibition by expressing shPERK in the cellular model did not alter almost any of the aspects studied, except the translation rate, which was significantly reduced.

We also verified that by removing the stress stimuli (SA), the levels of ataxin-2 and ataxin-3 were not re-established to control levels, but further experiments need to be performed, namely without PERKi treatment, as a control.

Finally, we observed that shPERK expression in the mouse striatum did not cause any neurotoxicity. But in a lentiviral mouse model of SCA3 (with the expression of mutant ataxin-3), the neuronal loss is significantly increased. This tells us that SGs induction might have a neuroprotective role in the context of the disease.

As a future study, we consider that it might be interesting to use pharmacologic PERK inhibition *in vivo* (PERKi treatment), upon these promising *in vitro* results. Study the PERK inhibition in a SCA2 mouse model, such as ataxin-2 was more altered in cellular models than ataxin-3. And performing more studies to understand the shPERK neurotoxicity in lentiviral SCA3 mouse model.

CHAPTER V – REFERENCES

ALBRECHT, Mario *et al.* - Structural and functional analysis of ataxin-2 and ataxin-3. **European Journal of Biochemistry**. . ISSN 00142956. 271:15 (2004) 3155–3170. Doi: 10.1111/j.1432-1033.2004.04245.x.

ALMEIDA, L. P. DE *et al.* - Neuroprotective effect of a CNTF-expressing lentiviral vector in the quinolinic acid rat model of Huntington's disease. **Neurobiol Dis**. . ISSN 0969-9961. 8:3 (2001) 433–446. Doi: 10.1006/nbdi.2001.0388.

ALVES, Sandro *et al.* - Striatal and nigral pathology in a lentiviral rat model of Machado-Joseph disease. **Human Molecular Genetics**. . ISSN 09646906. 17:14 (2008) 2071–2083. Doi: 10.1093/hmg/ddn106.

ALVES, Sandro *et al.* - Allele-specific RNA silencing of mutant ataxin-3 mediates neuroprotection in a rat model of Machado-Joseph disease. **Plos ONE**. . ISSN 19326203. 3:10 (2008). Doi: 10.1371/journal.pone.0003341.

AMOR, Sandra *et al.* - Inflammation in neurodegenerative diseases. **Immunology**. . ISSN 00192805. 129:2 (2010) 154–169. Doi: 10.1111/j.1365-2567.2009.03225.x.

ANDERSON, Paul; KEDERSHA, Nancy - Stressful initiations. **Journal of Cell Science**. 115:2002) 3227–3234.

ANDERSON, Paul; KEDERSHA, Nancy - RNA granules. **Journal of Cell Biology**. 172:6 (2006) 803–808. Doi: 10.1083/jcb.200512082.

ANDERSON, Paul; KEDERSHA, Nancy - Stress granules : the Tao of RNA triage. **Cell**. 33:2007) 141–150. Doi: 10.1016/j.tibs.2007.12.003.

ANDERSON, Paul; KEDERSHA, Nancy - Stress granules Primer Inhibition in cortical circuits. **Current Biology**. 19:C (2008) 397–398.

ANDERSON, Paul; KEDERSHA, Nancy - Stress granules Primer Inhibition in cortical circuits. **Current Biology**. 19:C (2009) 397–398.

ANDERSON, Paul; KEDERSHA, Nancy - RNA granules : post-transcriptional and epigenetic modulators of gene expression. **Nature Publishing Group**. . ISSN 1471-0072. 10:6 (2009) 430–436. Doi: 10.1038/nrm2694.

ARIMOTO, Kyoko *et al.* - Formation of stress granules inhibits apoptosis by suppressing stress-responsive MAPK pathways. **Nature cell biology**. 10:11 (2008) 1324–1332. Doi: 10.1038/ncb1791.

AVIVAR-VALDERAS, Alvaro *et al.* - PERK Integrates Autophagy and Oxidative Stress Responses To Promote Survival during Extracellular Matrix Detachment PERK Integrates Autophagy and Oxidative Stress Responses To Promote Survival during Extracellular Matrix Detachment. **Molecular and cellular biology**. . ISSN 1098-5549. 31:17 (2011) 3616–29. Doi: 10.1128/MCB.05164-11.

AXTEN, M. *Et al.* - Discovery of 7-Methyl-5-(1-{[3-(trifluoromethyl)phenyl]acetyl}-2,3-dihydro-1H-indol-5-yl)-7H-pyrrolo[2,3-d]pyrimidin-4-amine (GSK2606414), a Potent and Selective First-in-Class Inhibitor of Protein Kinase R (PKR)-like Endoplasmic Reticulum Kinase (PERK). **J. Med. Chem**. 55:2012) 7193–7207.

BAUMER, Dirk *et al.* - FTLD-ALS of TDP-43 type and SCA2 in a family with a full ataxin-2 polyglutamine expansion. **Acta Neuropathologica**. . ISSN 00016322. 2014). Doi: 10.1007/s00401-014-1277-z.

BENTMANN, Eva; HAASS, Christian; DORMANN, Dorothee - Stress granules in neurodegeneration – lessons learnt from TAR DNA binding protein of 43 kda and fused in sarcoma. **The FEBS journal**. 280:2013) 4348–4370. Doi: 10.1111/febs.12287.

BOSCO, Daryl A. *Et al.* - Mutant FUS proteins that cause amyotrophic lateral sclerosis incorporate into stress granules. **Human Molecular Genetics**. . ISSN 09646906. 19:21 (2010) 4160–4175. Doi: 10.1093/hmg/ddq335.

BUCHAN, J. Ross *et al.* - Eukaryotic stress granules are cleared by granulophagy and Cdc48 / VCP function. **Cell**. 153:7 (2013) 1461–1474.

BUCHAN, J. Ross - mrnp granules. **RNA biology**. . ISSN 1555-8584. 11:8 (2014) 1019–30. Doi: 10.4161/15476286.2014.972208.

BUCHAN, J. Ross; PARKER, Roy - Eukaryotic Stress Granules : The Ins and Out of Translation What are Stress Granules ? **Molecular Cell**. 36:6 (2013) 932–948.

CANDÉ, Céline *et al.* - Regulation of cytoplasmic stress granules by apoptosis-inducing factor. **Journal of Cell Science**. 117:19 (2004) 4461–4468. Doi: 10.1242/jcs.01356.

CASETTA, I.; GOVONI, V.; GRANIERI, E. - Oxidative stress, antioxidants and neurodegenerative diseases. **Curr.Pharm.Design**. . ISSN 1381-6128. 11:16 (2005) 2033–52. Doi: 10.2174/1381612054065729.

CHAN, S. H. U. Ning; TANG, B. O. R. Luen - Location and membrane sources for autophagosome formation – from ER-mitochondria contact sites to Golgi-endosome-derived

carriers. **Molecular Membrane Biology**. 30:8 (2013) 394–402. Doi: 10.3109/09687688.2013.850178.

CHOU, Kelvin L.; KOEPPE, Robert A.; BOHNEN, Nicolaas I. - Rhinorrhea: A common nondopaminergic feature of Parkinson's disease. **Movement Disorders**. . ISSN 08853185. 26:2 (2011) 320–323. Doi: 10.1002/mds.23366.

CHUDINOVA, E. M.; NADEZHDINA, E. S.; IVANOV, P. A. - Cellular Acidosis Inhibits Assembly , Disassembly , and Motility of Stress Granules. **Biochemestry**. 77:11 (2012) 1277–1284.

COHEN, Irun R. *Et al.* - **Advances in Experimental Medicine and Biology**. ISBN 9781461451068.

DABROWSKI, Maciej; BUKOWY-BIERYLLO, Zuzanna; ZIETKIEWICZ, Ewa - Translational readthrough potential of natural termination codons in eucaryotes – The impact of RNA sequence. **RNA biology**. 12:9 (2015) 950–958.

DEVER, Thomas E.; GREEN, Rachel - The Elongation, Termination, and Recycling Phases of Translation in Eukaryotes Thomas. **Cold Spring Harbor Laboratory Press**. 4:2012).

DING, Xunshan *et al.* - ALS-Associated Ataxin 2 polyq Expansions Enhance Stress- Induced Caspase 3 Activation and Increase TDP-43 Pathological Modifications. **Journal Neurosci.** . ISSN 1878-5832. 16:3 (2013) 387–393. Doi: 10.1016/j.cmet.2012.08.002.

DORMANN, Dorothee *et al.* - ALS-associated fused in sarcoma (FUS) mutations disrupt Transportin-mediated nuclear import. **The EMBO journal**. . ISSN 0261-4189. 29:16 (2010) 2841–2857. Doi: 10.1038/emboj.2010.143.

DURR, Alexandra - Autosomal dominant cerebellar ataxias: Polyglutamine expansions and beyond. **The Lancet Neurology**. . ISSN 14744422. 9:9 (2010) 885–894. Doi: 10.1016/S1474-4422(10)70183-6.

EICHLER, L. *Et al.* - Quantitative Assessment of Brain Stem and Cerebellar Atrophy in Spinocerebellar Ataxia Types 3 and 6 : Impact on Clinical Status. **Am J Neuroradiol**. 32:May (2011) 890–897. Doi: 10.3174/ajnr.A2387.

ELDEN, Andrew C. *Et al.* - Ataxin-2 intermediate-length polyglutamine expansions are associated with increased risk for ALS Andrew. **Nature**. 466:7310 (2011) 1069–1075. Doi: 10.1038/nature09320.Ataxin-2.

EMDE, Anna; HORNSTEIN, Eran - mirnas at the interface of cellular stress and disease. **The EMBO journal**. . ISSN 1460-2075. 33:13 (2014) 1428–37. Doi: 10.15252/embj.201488142.

GATCHEL, Jennifer R.; ZOGHBI, Huda Y. - focus on repeat in stability diseases of unstable repeat expansion : mechanisms and common principles. **Nature genetics**. 6:2005) 743–755. Doi: 10.1038/nrg1691.

GILKS, Natalie *et al.* - Stress Granule Assembly Is Mediated by Prion-like Aggregation of TIA-1. **Molecular Biology of the Cell**. 15:December (2004) 5383–5398. Doi: 10.1091/mbc.E04.

GOMES, Ligia C.; SCORRANO, Luca - Biochimica et Biophysica Acta Mitochondrial morphology in mitophagy and macroautophagy. **BBA - Molecular Cell Research**. . ISSN 0167-4889. 1833:1 (2013) 205–212. Doi: 10.1016/j.bbamcr.2012.02.012.

GOODMAN, Morris; BUILDING, Mcintyre - Could stress granules be involved in age - related diseases ? **AGING**. 1:9 (2009) 753–757.

GOWRISHANKAR, Gayatri *et al.* - Inhibition of mrna deadenylation and degradation by different types of cell stress. **Biol. Chem.** 387:March (2006) 323–327. Doi: 10.1515/BC.2006.043.

GUEVARA-GARCIA, M. *Et al.* - Oxidative stress as a cofactor in spinocerebellar ataxia type 2. **Redox Report**. . ISSN 1351-0002 1743-2928. 17:2 (2012) 84–89. Doi: http://dx.doi.org/10.1179/84 1351000212Y.0000000005.

HALLIDAY, M. *Et al.* - Partial restoration of protein synthesis rates by the small molecule ISRIB prevents neurodegeneration without pancreatic toxicity. **Cell Death and Disease**. . ISSN 2041-4889. 6:3 (2015) e1672. Doi: 10.1038/cddis.2015.49.

HASEGAWA, Masato *et al.* - Ubiquitinated TDP-43 in Frontotemporal Lobar Degeneration and Amyotrophic Lateral Sclerosis. **Annals of Neurology**. . ISSN 03645134. 64:1 (2008) 60–70. Doi: 10.1002/ana.21425.

HEIN, Nadine *et al.* - The nucleolus : an emerging target for cancer therapy. **Trends in Molecular Medicine**. . ISSN 1471-4914. 2013) 1–12. Doi: 10.1016/j.molmed.2013.07.005.

HILGERS, R. I. E.; TEIXEIRA, Daniela; PARKER, R. O. Y. - Translation-independent inhibition of mrna deadenylation during stress in Saccharomyces cerevisiae. **RNA**. 12:2006) 1835–1845. Doi: 10.1261/rna.241006.stress.

HINNEBUSCH, Alan G. - The Scanning Mechanism of Eukaryotic Translation Initiation. **ARI**. 83:January (2014) 1–34. Doi: 10.1146/annurev-biochem-060713-035802.

HOFMANN, Sarah *et al.* - Translation suppression promotes stress granule formation and cell survival in response to cold shock. **Molecular Biology of the Cell**. 23:2012) 3786–3800. Doi: 10.1091/mbc.E12-04-0296.

HUYNH, D. P. *Et al.* - Nuclear localization or inclusion body formation of ataxin-2 are not necessary for SCA2 pathogenesis in mouse or human. TL - 26. **Nature genetics**. . ISSN 1061-4036. 26 VN - r:1 (2000) 44–50. Doi: 10.1038/79162.

HUYNH, Duong P. *Et al.* - Expansion of the polyq repeat in ataxin-2 alters its Golgi localization , disrupts the Golgi complex and causes cell death. **Human Molecular Genetics**. 12:13 (2003) 1485–1496. Doi: 10.1093/hmg/ddg175.

HUYNH, Duong P. *Et al.* - Expansion of the polyq repeat in ataxin-2 alters its Golgi localization, disrupts the Golgi complex and causes cell death. **Human Molecular Genetics**. . ISSN 09646906. 12:13 (2003) 1485–1496. Doi: 10.1093/hmg/ddg175.

JACKSON, Richard J.; HELLEN, Christopher U. T.; PESTOVA, Tatyana V - The mechanism of eukaryotic translation initiation and principles of its regulation. **Nature Reviews**. 10:february (2010) 113–127. Doi: 10.1038/nrm2838.

KAPP, Lee D.; LORSCH, Jon R. - E UKARYOTIC T RANSLATION. **Annu. Rev. Biochem.** 73:2004) 657–704. Doi: 10.1146/annurev.biochem.73.030403.080419.

KAYALI, F.; MONTIE, H. L.; RAFOLS, J. A. - prolonged translation arrest in reperfused hippocampal cornu ammonis 1 is mediated by stress granules. **Neuroscience**. 134:2005) 1223–1245. Doi: 10.1016/j.neuroscience.2005.05.047.

KEDERSHA, N.; ANDERSON, P. - Stress granules : sites of mrna triage that regulate mrna stability Stress granules (sgs): a historical perspective. **Biochemical Society Tramsactions**. 30:2002) 963–969.

KEDERSHA, Nancy *et al.* - Dynamic Shuttling of TIA-1 Accompanies the Recruitment of mrna to Mammalian Stress Granules 7. **Journal of Cell Biology**. 151:6 (2000) 1257–1268.

KEDERSHA, Nancy *et al.* - Stress granules and processing bodies are dynamically linked sites of mrnp remodeling 4. **Journal of Cell Biology**. 169:6 (2005) 871–884. Doi: 10.1083/jcb.200502088.

KEDERSHA, Nancy - Relationship of GW/P-Bodies with Stress Granules. **Adv Exp Med Biol.** 768:2015) 197–211. Doi: 10.1007/978-1-4614-5107-5.

KEDERSHA, Nancy; ANDERSON, Paul - Mammalian Stress Granules and Processing Bodies. **Elsevier Inc.** 431:07 (2007) 61–81. Doi: 10.1016/S0076-6879(07)31005-7.

KEDERSHA, Nancy L. *Et al.* - RNA-binding Proteins TIA-1 and TIAR Link the Phosphorylation of eif-2alpha to the Assembly of Mammalian Stress Granules. **Journal of Cell Biology**. 147:7 (1999) 1431–1441.

KIM, Hyung-jun *et al.* - TDP-43 toxicity in amyotrophic lateral sclerosis disease models. **Nature genetics**. 46:2 (2014) 152–160. Doi: 10.1038/ng.2853.Therapeutic.

KLIONSKY, Daniel J.; ESKELINEN, Eeva-liisa; DERETIC, Vojo - Autophagosomes, phagosomes, autolysosomes, phagolysosomes, autophagolysosomes… Wait, I'm confused. **Autophagy**. 10:April (2014) 549–551.

KLOCKGETHER, Ullrich Wüllner; Michael Reimold; Michael Abele; Katrin Bürk; Martina Minnerop; Bernd-Michael Dohmen; Hans-Juergen Machulla; Roland Bares; Thomas - Dopamine Transporter Positron Emission Tomography in Spinocerebellar Ataxias Type 1, 2, 3, and 6. **Arch Neurol.** 62:2005) 1280–1285.

KOYANO, Shigeru *et al.* - Neuronal intranuclear inclusions in spinocerebellar ataxia type 2: Triple-labeling immunofluorescent study. **Neuroscience Letters**. . ISSN 03043940. 273:2 (1999) 117–120. Doi: 10.1016/S0304-3940(99)00656-4.

LEE, Ji Ann; TANG, Zhen Zhi; BLACK, Douglas L. - An inducible change in Fox-1/A2BP1 splicing modulates the alternative splicing of downstream neuronal target exons. **Genes and Development**. . ISSN 08909369. 23:19 (2009) 2284–2293. Doi: 10.1101/gad.1837009.

LI, Yun R. *Et al.* - Stress granules as crucibles of ALS pathogenesis. **Journal of Cell Biology**. 201:3 (2013) 361–372. Doi: 10.1083/jcb.201302044.

LIU, Baohua; ZHOU, Zhongjun; LAM, Yun W. - Quantitative nucleolar proteomics reveals nuclear re-organization during stress- induced senescence in mouse fibroblast. **BMC Cell Biology**. . ISSN 1471–2121. 12:1 (2011) 33. Doi: 10.1186/1471-2121-12-33.

LIU-YESUCEVITZ, Liqun *et al.* - Tar DNA binding protein-43 (TDP-43) associates with stress granules: Analysis of cultured cells and pathological brain tissue. **Plos ONE**. . ISSN 19326203. 5:10 (2010). Doi: 10.1371/journal.pone.0013250.

LLOYD, Richard E. - How Do Viruses Interact with Stress-Associated RNA Granules ? **Plos Pathogens**. 8:6 (2012) 6–9. Doi: 10.1371/journal.ppat.1002741.

LOO, Simone VAN DE *et al.* - Ataxin-2 associates with rough endoplasmic reticulum. **Experimental Neurology**. . ISSN 00144886. 215:1 (2009) 110–118. Doi: 10.1016/j.expneurol.2008.09.020.

MAGAÑA, J. J.; VELÁZQUEZ-PÉREZ, L.; CISNEROS, B. - Spinocerebellar ataxia type 2: Clinical presentation, molecular mechanisms, and therapeutic perspectives. **Molecular Neurobiology**. . ISSN 08937648. 47:1 (2013) 90–104. Doi: 10.1007/s12035-012-8348-8.

MAHBOUBI, Hicham; STOCHAJ, Ursula - Nucleoli and Stress Granules : Connecting Distant Relatives. **Traffic**. 15:10 (2014) 1179–1193. Doi: 10.1111/tra.12191.

MANGIARDI, Dominic A. *Et al.* - Progression of Hair Cell Ejection and Molecular Markers of Apoptosis in the Avian Cochlea following Gentamicin Treatment. **The Journal of comparative Neurology**. 475:October 2003 (2004) 1–18. Doi: 10.1002/cne.20129.

MARIAPPAN, Meenalakshmi M. *Et al.* - Ribosomal biogenesis induction by high glucose requires activation of upstream binding factor in kidney glomerular epithelial cells. **AJP-Renal Physiol**. 300:2011) 219–230. Doi: 10.1152/ajprenal.00207.2010.

MATILLA-DUEÑAS, Antoni *et al.* - machado-joseph disease and other rare spinocerebellar ataxias. **Neurodegenerative Diseases**. 2012) 172–188.

MATOS, Carlos A. *Et al.* - Ataxin-3 phosphorylation decreases neuronal defects in spinocerebellar ataxia type 3 models. **Journal of Cell Biology**. . ISSN 15408140. 212:4 (2016) 465–480. Doi: 10.1083/jcb.201506025.

MAZROUI, Rachid *et al.* - Inhibition of the Ubiquitin-Proteasome System Induces Stress Granule Formation. **Molecular Biology of the Cell**. 18:July (2007) 2603–2618. Doi: 10.1091/mbc.E06.

MERCHANT, Michael L. *Et al.* - Urinary Peptidome May Predict Renal Function Decline in Type 1 Diabetes and Microalbuminuria. **J Am soc Nephrol**. 20:2009) 2065–2074. Doi: 10.1681/ASN.2008121233.

MOELLER, Benjamin J. *Et al.* - Radiation activates HIF-1 to regulate vascular radiosensitivity in tumors : Role of reoxygenation , free radicals , and stress granules. **Cancer Cell**. 5:May (2004) 429–441.

MONAHAN, Zachary; SHEWMAKER, Frank; BHAN, Udai - Stress granules at the intersection of autophagy and ALS. **Brain Research**. . ISSN 0006-8993. 2016) 1–12. Doi: 10.1016/j.brainres.2016.05.022.

MOUAIKEL, John; GEER, Peter VANDER; TAZI, Jamal - rasgap-Associated Endoribonuclease G3BP : Selective RNA Degradation and Phosphorylation-Dependent Localization. **Molecular and cellular biology**. 21:22 (2001) 7747–7760. Doi: 10.1128/MCB.21.22.7747.

NASCIMENTO-FERREIRA, Isabel *et al.* - Overexpression of the autophagic beclin-1 protein clears mutant ataxin-3 and alleviates Machado-Joseph disease. **Brain**. . ISSN 00068950. 134:5 (2011) 1400–1415. Doi: 10.1093/brain/awr047.

NATHANS, D. - Puromycin Inhibition of Protein Synthesis: Incorporation of Puromycin Into Peptide Chains. **Proceedings of the National Academy of Sciences of the United States of America**. . ISSN 0027-8424. 51:1963 (1964) 585–92.

NIXON, Ralph A. *Et al.* - Extensive Involvement of Autophagy in Alzheimer Disease: An Immuno-Electron Microscopy Study. **Journal of Neuropathology & Experimental Neurology**. . ISSN 0022-3069. 64:2 (2005) 113–122. Doi: 10.1093/jnen/64.2.113.

NÓBREGA, Clévio *et al.* - Re-establishing ataxin-2 downregulates translation of mutant ataxin-3 and alleviates Machado-Joseph disease. **Brain**. . ISSN 14602156. 138:12 (2015) 3537–3554. Doi: 10.1093/brain/awv298.

NONHOFF, Ute *et al.* - Ataxin-2 Interacts with the DEAD / H-Box RNA Helicase DDX6 and Interferes with P-Bodies and Stress Granules. **Molecular Biology of the Cell**. 18:April (2007) 1385–1396. Doi: 10.1091/mbc.E06.

Ö. ALTUG-TEBER, M. BONIN, M. WALTER, U.A. MAU-HOLZMANN, A. DUFKE, H. STAPPERT, I. TEKESIN, H. HEILBRONNER, K. NIESELT, O. Riess - Specific transcriptional changes in human fetuses with autosomal trisomies. **Cytogenet Genome Research**. 184:2007 (2008) 171–184. Doi: 10.1159/000112058.

ORR, Harry T.; ZOGHBI, Huda Y. - Trinucleotide Repeat Disorders. **Annual Review of Neuroscience**. 30:2007) 575–623. Doi: 10.1146/annurev.neuro.29.051605.113042.

PANG, Joanna T. *Et al.* - Neuronal intranuclear inclusions in SCA2: a genetic, morphological and immunohistochemical study of two cases. **Brain : a journal of neurology**. . ISSN 0006-8950. 125:Pt 3 (2002) 656–663. Doi: 10.1093/brain/awf060.

PASTORE, Annalisa; BAUER, Peter; SCHO, Ludger - SCA3 : Neurological features , pathogenesis and animal models. **The Cerebellum**. March (2008) 125–137.

PAULSON, Henry - Machado-Joseph Disease/Spinocerebellar Ataxia Type 3. **Handb Clin Neurol.** 103: (2013) 437–449. Doi: 10.1016/B978-0-444-51892-7.00027-9.Machado-Joseph.

PAULSON, Henry L.; PH, D. - Dominantly Inherited Ataxias : Lessons Learned from Machado-Joseph Disease / Spinocerebellar Ataxia Type 3. **Seminars in Neurology**. 27:212 (2007) 133–142. Doi: 10.1055/s-2007-971172.

PAULSON, Maria Do Carmo Costa And Henry L. - Toward understanding Machado-Joseph Disease Maria. **Prog Neurobiol.** 97:2 (2013) 239–257. Doi: 10.1016/j.pneurobio.2011.11.006.Toward.

PROUDFOOT, Nick J. - polymerase II juggernaut. **Science**. 352:2016) 1291–1301. Doi: 10.1126/science.

PULST, Stefan M. - Spinocerebellar Ataxia 2 (SCA2). **Genetics of Movement Disorders**. . ISSN 14734222. 2:April (2003) 45–56. Doi: 10.1016/B978-012566652-7/50006-X.

RALSER, Markus *et al.* - An integrative approach to gain insights into the cellular function of human ataxin-2. **Journal of Molecular Biology**. . ISSN 00222836. 346:1 (2005) 203–214. Doi: 10.1016/j.jmb.2004.11.024.

RUSTEN, Tor Erik; STENMARK, Harald - P62, an Autophagy Hero or Culprit? **Nature cell biology**. . ISSN 1465-7392. 12:3 (2010) 207–209. Doi: 10.1038/ncb0310-207.

SATTERFIELD, Terrence F.; PALLANCK, Leo J. - Ataxin-2 and its Drosophila homolog, ATX2, physically assemble with polyribosomes. **Human Molecular Genetics**. . ISSN 09646906. 15:16 (2006) 2523–2532. Doi: 10.1093/hmg/ddl173.

SCHEEL, Hartmut *et al.* - Elucidation of ataxin-3 and ataxin-7 function by integrative bioinformatics. **Human Molecular Genetics**. 12:21 (2003) 2845–2852. Doi: 10.1093/hmg/ddg297.

SCHEPER, Wiep; HOOZEMANS, Jeroen J. M. - A new perkspective on neurodegeneration. **Science translational medicine**. . ISSN 1946-6242. 5:206 (2013) 206fs37. Doi: 10.1126/scitranslmed.3007641.

SEIDEL, Kay *et al.* - On the distribution of intranuclear and cytoplasmic aggregates in the brainstem of patients with spinocerebellar ataxia type 2 and 3. **Brain Pathology**. . ISSN 10156305. 2016). Doi: 10.1111/bpa.12412.

SHAO, Jieya; DIAMOND, Marc I. - Polyglutamine diseases : emerging concepts in pathogenesis and therapy. **Human Molecular Genetics**. 16:2 (2007) 115–123. Doi: 10.1093/hmg/ddm213.

SWISHER, Kylie D.; PARKER, Roy - Localization to, and effects of Pbp1, Pbp4, Lsm12, Dhh1, and Pab1 on stress granules in Saccharomyces cerevisiae. **Plos ONE**. . ISSN 19326203. 5:4 (2010) 1–14. Doi: 10.1371/journal.pone.0010006.

TAKAO, Masaki *et al.* - Spinocerebellar ataxia type 2 is associated with Parkinsonism and Lewy body pathology. **BMJ case reports**. . ISSN 1757-790X. 2011:2011) 22–25. Doi: 10.1136/bcr.01.2011.3685.

TAKBUM OHN, NANCY KEDERSHA, TYLER HICKMAN, SARAH TISDALE, And Paul Anderson - A functional rnai screen links O-glcnac modification of ribosomal proteins to stress granule and processing body assembly. **Nature cell biology**. 10:10 (2008) 1224–1231. Doi: 10.1038/ncb1783.A.

TSAI, Nien-pei; HO, Ping-chih; WEI, Li-na - Regulation of stress granule dynamics by Grb7 and FAK signalling pathway. **The EMBO journal**. 27:5 (2008) 715–726. Doi: 10.1038/emboj.2008.19.

TURNBULL, Victor J. *Et al.* - Different ataxin-2 antibodies display different immunoreactive profiles. **Brain Research**. . ISSN 00068993. 1027:1-2 (2004) 103–116. Doi: 10.1016/j.brainres.2004.08.044.

UCHIHARA, Toshiki *et al.* - Non-expanded polyglutamine proteins in intranuclear inclusions of hereditary ataxias – triple-labeling immunofluorescence study. **Acta Neuropathologica**. 102:2001) 149–152. Doi: 10.1007/s004010100364.

VANDERWEYDE, Tara *et al.* - Contrasting pathology of the stress granule proteins TIA-1 and G3BP in tauopathies. **The Journal of neuroscience : the official journal of the Society for Neuroscience**. . ISSN 1529-2401. 32:24 (2012) 8270–83. Doi: 10.1523/JNEUROSCI.1592-12.2012.

VELÁZQUEZ PÉREZ, Luis *et al.* - Electrophysiological features in patients and presymptomatic relatives with spinocerebellar ataxia type 2. **Journal of the Neurological Sciences**. . ISSN 0022510X. 263:1-2 (2007) 158–164. Doi: 10.1016/j.jns.2007.07.013.

VELÁZQUEZ-PÉREZ, L. *Et al.* - Saccade velocity is reduced in presymptomatic spinocerebellar ataxia type 2. **Clinical Neurophysiology**. . ISSN 13882457. 120:3 (2009) 632–635. Doi: 10.1016/j.clinph.2008.12.040.

VELAZQUEZ-PEREZ, Luis *et al.* - Progression markers of Spinocerebellar Ataxia 2. A twenty years neurophysiological follow up study. **Journal of the Neurological Sciences**. . ISSN 0022510X. 290:1-2 (2010) 22–26. Doi: 10.1016/j.jns.2009.12.013.

VELÁZQUEZ-PÉREZ, Luis *et al.* - Saccade velocity is controlled by polyglutamine size in spinocerebellar ataxia 2. **Annals of Neurology**. ISSN 03645134. 56:3 (2004) 444–447. Doi: 10.1002/ana.20220.

WADIA, N. H.; SWAMI, R. K. - A new form of heredo-familial spinocerebellar degeneration with slow eye movements (nine families). **Brain**. . ISSN 00068950. 94:2 (1971) 359–374. Doi: 10.1093/brain/94.2.359.

WINBORN, Brett J. *Et al.* - The Deubiquitinating Enzyme Ataxin-3 , a Polyglutamine Disease Protein , Edits Lys 63 Linkages in Mixed Linkage Ubiquitin Chains. **The Journal of Biological Chemistry**. 283:39 (2008) 26436–26443. Doi: 10.1074/jbc.M803692200.

WIPPICH, Frank *et al.* - Dual Specificity Kinase DYRK3 Couples Stress Granule Condensation / Dissolution to mtorc1 Signaling. **Cell**. . ISSN 0092-8674. 152:4 (2013) 791–805. Doi: 10.1016/j.cell.2013.01.033.

WOLOZIN, Benjamin - Regulated protein aggregation: stress granules and neurodegeneration. **Molecular neurodegeneration**. . ISSN 1750-1326. 7:1 (2012) 56. Doi: 10.1186/1750-1326-7-56.

WOLOZIN, Benjamin - Physiological protein aggregation run amuck: stress granules and the genesis of neurodegenerative disease. **Discovery medicine**. . ISSN 1944-7930. 17:91 (2014) 47–52.

ZOGHBI, Huda Y.; ORR, Harry T. - glutamine repeats and neurodegeneration **Annu. Rev. Neurosci.** 23:2000) 217–247.